



Anjani Parsotamo

Bachelor of Science in Chemical and Biochemical
Engineering

Performance of Mobile Biological Attached Growth Systems

Dissertation to obtain the degree of Master in Chemical and
Biochemical Engineering

Supervisor: Ana Soares, Cranfield University, Cranfield, UK



September 2017

This page was intentionally left blank



Anjani Parsotamo

Bachelor of Science in Chemical and Biochemical
Engineering

Performance of Mobile Biological attached growth Systems

Dissertation to obtain the degree of Master in Chemical and
Biochemical Engineering

Supervisor: Ana Soares, Cranfield University, Cranfield, UK

FCT FACULDADE DE
CIÊNCIAS E TECNOLOGIA
UNIVERSIDADE NOVA DE LISBOA

September 2017

This page was intentionally left blank

Performance of Mobile Biological Attached Growth Systems

Copyright © Anjani Parsotamo, Faculdade de Ciências e Tecnologia, Universidade Nova de Lisboa.

A Faculdade de Ciências e Tecnologia e a Universidade Nova de Lisboa têm o direito, perpétuo e sem limites geográficos, de arquivar e publicar esta dissertação através de exemplares impressos reproduzidos em papel ou de forma digital, ou por qualquer outro meio conhecido ou que venha a ser inventado, e de a divulgar através de repositórios científicos e de admitir a sua cópia e distribuição com objetivos educacionais ou de investigação, não comerciais, desde que seja dado crédito ao autor e editor.

This page was intentionally left blank

This page was intentionally left blank

Agradecimentos

A realização desta dissertação de mestrado contou com importantes apoios e incentivos sem os quais não se teria tornado uma realidade e aos quais estarei eternamente grata.

Por esta razão, desejo expressar os meus sinceros agradecimentos:

Primeiramente agradeço ao professor Mário Eusébio, pelo acompanhamento e disponibilidade apresentada ao longo de todo curso, e à professora Ascensão por ter providenciado a oportunidade de acabar a minha tese de mestrado em Cranfield University.

Agradeço á minha orientadora Ana Soares pela oportunidade e o privilégio me dado em me ter inserido no doutoramento da Joana. e por todo o apoio me dado ao longo destes últimos seis meses.

Agradeço profundamente à minha coorientadora, Joana Dias por toda a confiança depositada em mim, também pela oportunidade me dada por ter inserido no seu projeto de doutoramento e especialmente por todo o apoio me dado ao longo da escrita da tese, que foi até ao ultimo dia incansável.

Agradeço a todos os meus amigos e colegas da faculdade por todo o apoio e companhia, principalmente à Ilaria Negrin pelo seu apoio incansável nos meus últimos dias em Cranfield, e ao Jan Vandenwegue pelo seu apoio incondicional na escrita desta dissertação.

Por fim, aos meus pais que possibilitaram com que este sonho se tornasse realidade, um sincero obrigado.

This page was intentionally left blank

“A ciência nunca resolve um problema sem criar pelo menos outros dez”.

George Bernard Shaw

This page was intentionally left blank

Abstract

This project aimed at investigating the treatment performance of a pilot-scale mobile attached growth system (moving bed biofilm reactor (MBBR) /suspended aerated filter (SAF)), using a spherical carrier media (Media 1) with a protected surface area of $112 \text{ m}^2 \cdot \text{m}^{-3}$. The pilot scale reactor had a volume of 2 m^3 and it was fed continuously with settled wastewater coming from a full-scale municipal wastewater treatment plant (WWTP). Different organic loads were applied to study the efficiency of organic and ammonia removal and to understand what was the maximum organic loading rates that could be applied. The study was carried out for a period of six months.

The organic loadings applied were 6, 8 12 and $16 \text{ g m}^{-2} \text{ d}^{-1}$. For organic loads of $12 \text{ g COD m}^{-2} \text{ d}^{-1}$ the soluble COD removal efficiency ranged from $38 \pm 11\%$, corresponding to surface loading rate $2.35 \pm 0.8 \text{ g COD m}^{-2} \text{ d}^{-1}$ and removal rate of $0.9 \pm 0.6 \text{ g COD m}^{-2} \text{ d}^{-1}$. The soluble BOD, removal efficiency ranged from $92 \pm 4\%$, corresponding to surface loading rate of $0.61 \pm 0.20 \text{ BOD m}^{-2} \text{ d}^{-1}$ and removal rate of $0.57 \pm 0.21 \text{ g BOD m}^{-2} \text{ d}^{-1}$. The nitrification, efficiency ranged from $65 \pm 22\%$, corresponding to loading rate of $0.86 \pm 0.16 \text{ g N-NH}_4^+ \text{ m}^{-2} \text{ d}^{-1}$ and removal rate of $0.63 \pm 0.19 \text{ g N-NH}_4^+ \text{ m}^{-2} \text{ d}^{-1}$.

The second part of the project aimed to determining the external mass transfer and the boundary layer thickness of the biofilm developed in media with different protected surface areas ($112 \text{ m}^2 \cdot \text{m}^{-3}$ - Media 1, $220 \text{ m}^2 \cdot \text{m}^{-3}$ - Media 2 and $348 \text{ m}^2 \cdot \text{m}^{-3}$ - Media 3). A lab scale MBBR/SAF with a volume of 30L containing the media (with biofilm) and wastewater was subjected to different mixing intensities. The mass transfer coefficient and boundary layer thickness obtained ranged from $2.77 - 4.90 \text{ m d}^{-1}$ and $35.53 - 85.81 \text{ }\mu\text{m}$ for Media 1, from $2.24 - 15.61 \text{ m d}^{-1}$ and $11.14 - 77.5 \text{ }\mu\text{m}$ for Media 2 and, from $1.80 - 15.90 \text{ m d}^{-1}$ and $11.0 - 96.73 \text{ }\mu\text{m}$ for Media 3, respectively.

Keywords: Wastewater treatment, mobile attached growth, organic matter, ammonia oxidation, removal efficiency, mass transfer coefficient, boundary layer thickness.

This page was intentionally left blank

Resumo

O presente trabalho teve como objetivo o estudo da eficiência de um sistema leito móvel (*moving bed biological system*, *MBBR* e *submerged aeraed filters*, *SAF*) para tratamento de águas residuais.

Foi usado um MBBR/SAF reator de 2 m³ de volume, alimentado continuamente com água residual proveniente da estação de tratamento de águas de *Cranfield University*. Este estudo foi realizado em escala piloto, usando um suporte de plástico (Media 1) com área de superfície de 112 m².m⁻³. Este estudo foi realizado num período de seis meses. Diferentes cargas orgânicas foram aplicadas de modo a estudar a eficiência de remoção orgânica e a eficiência de remoção de amônia para determinar a máxima carga orgânica que o sistema consegue obter operar de modo a obter rendimento máximo.

Uma carga inicial de 6 g m⁻² d⁻¹ foi aplicada e aumentada gradualmente para 8, 12 e 10 16 g m⁻² d⁻¹. Para a carga orgânica onde a eficiência foi obtida foi maior, 12 g COD m⁻² d⁻¹, os valores obtidos foram: CQO (carência química de oxigénio) solúvel a eficiência de remoção foi de 38 ± 11%, a carga orgânica de 2.35 ± 0.8 g CQO m⁻² d⁻¹ e a taxa de remoção foi de 0.9 ± 0.6 g CQO m⁻² d⁻¹; CBO (carência bioquímica de oxigénio) solúvel a eficiência de remoção foi de 92% ± 4, a carga orgânica de 0.61 ± 0.20 g CBO m⁻² d⁻¹ e a taxa de remoção de 0.57 ± 0.21 g CBO m⁻² d⁻¹; nitrificação a eficiência de remoção foi de 65% ± 22, a carga orgânica de 0.86 ± 0.16 g N-NH₄⁺ m⁻² d⁻¹ e taxa de remoção 0.63 ± 0.19 g N-NH₄⁺ m⁻² d⁻¹.

A segunda parte deste trabalho consistiu em determinar o coeficiente de transferência de massa externa e a espessura da camada limite. Foi usado o reator MBBR/SAF á escala laboratorial, com um volume de 30L operando em modo *batch*. Foram aplicadas diferentes intensidades de mistura para o estudo do coeficiente de transferência de massa para três tipos de medias com área de superfície diferentes (112 m².m⁻³ - Media 1, 220 m².m⁻³ - Media 2 e 348 m².m⁻³ - Media 3).

Os resultados obtidos para o coeficiente de transferência de massa e a espessura da camada limite foram: de 2.77 – 4.89 m d⁻¹ e 35.53 – 85.81 µm para Media 1, de 2.24 – 15.61 m d⁻¹ e 11.14 – 77.5 µm para Media 2 e, de 1.80 – 15.90 m d⁻¹ e 10.95 – 96.73 µm para Media 3, respetivamente.

Palavras Chaves: Wastewater treatment, mobile attached growth, organic matter, ammonia oxidation, removal efficiency, mass transfer coefficient, boundary layer thickness.

This page was intentionally left blank

Table of Contents

| | |
|--|-----|
| Agradecimientos..... | i |
| Abstract | v |
| Resumo..... | vii |
| 1. Introduction | 1 |
| 2. Objectives..... | 7 |
| 3. Material and Methods..... | 9 |
| 3.1 Media Studied | 9 |
| 3.2 Pilot-scale MBBR/SAF technology performance experiments..... | 10 |
| 3.3 Organic loading rates increase | 11 |
| 3.4 External mass transfer experiments..... | 11 |
| 3.5 Analytical methods..... | 13 |
| 4. Results and Discussion..... | 19 |
| 4.1 SAF performance study for Media 1..... | 19 |
| 4.2 External Mass Transfer coefficient determination | 32 |
| 5. Conclusion..... | 39 |
| 6. References | 41 |
| 7. Appendix | 45 |
| 7.1 Appendix I..... | 45 |
| 7.2 Appendix II | 49 |
| 7.3 Appendix III | 51 |
| 7.4 Appendix IV | 53 |
| 7.5 Appendix V | 52 |

List of Figures

| | |
|--|----|
| Figure 1.1 - Attached processes for biological wastewater treatment. [11] | 3 |
| Figure 1.2-Biofilm development stages. Stage 1 Initial attachment, Stage 2- Irreversibly attachment, Stage 3- EPS formation, Stage 4- maturation and Stage 5- dispersal. ¹⁹ | 5 |
| Figure 1.3 – Schematic representation of biofilm structure. ²⁰ | 6 |
| Figure 1.4- Substrate concentration consumption throughout the biofilm thickness at different stages. ²² | 6 |
| Figure 3.1- Pilot scale MBBR/SAF reactor used in study case..... | 10 |
| Figure 3.2- Scheme of MBBR/SAF used in this study case. | 11 |
| Figure 3.3- Lab-scale MBBR/SAF used in this study case. | 11 |
| Figure 3.4- Schematic variation of the substrate removal rate. The mixing intensity is increased until no effects of external mass transfer coefficient is observed in removal rate . ¹⁶ | 12 |
| Figure 4.1- Biomas density growth variation obtanaied from cell 1, cell 2 and cell3 at differet OLRs applied. Stage 1 – day 0 to 60 Stage 2 – day 61 to 101, Stage 3- day 102 to 126 and Stage 4- day 127 to 136..... | 21 |
| Figure 4.2- Removal OLR of sCOD and tCOD ($\text{gCOD m}^{-2} \text{d}^{-1}$) versus time (days). Stage 1 – day0 to 63, stage 2 – day 64 to100, stage 3- day 101 to 126 and stage 4- day 127 to 140. | 23 |
| Figure 4.3- tCOD lading rate ($\text{g tCOD m}^{-2} \text{d}^{-1}$) vesus obtainable removal rate ($[\text{g tCODin} - \text{g sCOD out}] \text{m}^{-2} \text{d}^{-1}$)..... | 25 |
| Figure 4.4- tBOD and sBOD removal ($\text{gBOD m}^{-2} \text{d}^{-1}$) versus time (days) for different OLRs applied. Stage 1 – day 0 to 58, stage 2 – day 59 to 98, stage 3- day 99 to 121 and stage 4- day 122 to 134..... | 27 |
| Figure 4.5- Inlet and Outlet of ammonium concentrations at different OLRs. Stage 1 – day0 to 60, stage 2 – day 61 to98, stage 3- day 98 to 126 and stage 4- day 127 to 14 | 28 |
| Figure 4.6- Amonia removal rate as function of amonia loads. For different OLRs applied..... | 29 |
| Figure 4.7- Poteins quantification evaluated as function of time, expressed at the specif weight, mgPN/gMLVSS | 31 |
| Figure 4.8- Carbohydrates quantification evaluates as function of tima, at the specfic weight mgPS/gMLVSS..... | 31 |
| Figure 4.9- Difference of sCOD concentration obtained as function of time, for Media 1(4.9- a), Media2 (4.9-b) and Media 3 (4.9-c) for the lowest mixing intensity. | 32 |
| Figure 4.10 – COD Removal rates obtabied as function of vvm for Media 1, Media 2 and Media 3 | 34 |

| | |
|---|----|
| Figure 4.11- Boundary layer thickness obtained from Media 1,2 and at different mixing intensities, when sCOD conversion is no longer affected by mixing intensity..... | 34 |
| Figure 4.12- Scan image obtained from OCT microprobe for measurement of biofilm thickness..... | 35 |
| Figure 4.13- External Mass Transfer obtained from Media 1, Media 2 and Media 3. | 36 |
| Figure 7.1- pH variation obtained for inlet and outlet at different OLRs..... | 49 |
| Figure 7.2- Evaluation of the temperature within the reactor for a frame time of six months, for cell 1, cell 2 and cell3..... | 49 |
| Figure 7.3- Dissolved Oxygen variation obtained for cell 1, cell 2 and cell 3, at different OLRs. | 49 |
| Figure 7.4- Total COD concentration removal efficiency (mgL^{-1}) versus time (days) for different OLRs. Stage 1 – day 0 to 63, stage 2 – day 64 to 100, stage 3- day 101 to 126 and stage 4- day 127 to 140..... | 51 |
| Figure 7.5- Soluble COD concentration removal efficiency (mgL^{-1}) versus time (days) for different OLRs. Stage 1 – day 0 to 63, stage 2 – day 64 to 100, stage 3- day 101 to 126 and stage 4- day 127 to 140..... | 51 |
| Figure 7.6 - Total BOD concentration removal efficiency (mgL^{-1}) versus time (days) at different OLRs. Stage 1 – day 0 to 58, stage 2 – day 59 to 98, stage 3- day 99 to 121 and stage 4- day 122 to 134..... | 52 |
| Figure 7.7- Total BOD concentration removal efficiency (mgL^{-1}) versus time (days) at different OLRs. Stage 1 – day 0 to 58, stage 2 – day 59 to 98, stage 3- day 99 to 121 and stage 4- day 122 to 134..... | 52 |
| Figure 7.8- Difference of sCOD concentration obtained as function of time, for Media 1 at different mixing intensities 3.5 vvm Fig.7.8- a, 5 vvm Fig.7.8- b, 7.5 vvm Fig.7.8- c, 10 vvm Fig.7.8- d, 15 vvm Fig.7.8- e, 25 vvm Fig.7.8- f. | 53 |
| Figure- 7.9 Difference of sCOD concentration obtained as function of time, for Media 2 at different mixing intensities 2.5 vvm Fig.7.9 – a, 3.5 vvm Fig.7.9- b, 10 vvm Fig.7.9- c, 15 vvm Fig.7.9- d, 20 vvm Fig.7.9- e, 30 vvm Fig.7.9-f. | 54 |
| Figure 7.10- Examples of scan images obtained for biofilm thickness measurements. Fig. 7.10-a, Fig. 7.10-b and Fig. 7.10-c | 52 |
| Figure 7.11- Attached biomass Media 1 | 53 |
| Figure 7.12- Attached biomass Media 2. | 53 |
| Figure 7.13- Attached biomass Media 3. | 54 |
| Figure 7.14- Lab scale reactor with Media 3..... | 54 |

List of Tables

| | |
|--|----|
| Table 3.1 - Media carriers used for the performance study of MBBR/SAF technology..... | 9 |
| Table 3.2- Physical properties of studied medias..... | 9 |
| Table 4.1- Influent wastewater characterization (after pre-treatment within six months timeframe). | 19 |
| Table 4.2- OLRs, flow rates conditions and HRT applied in MBBR/SAF..... | 20 |
| Table 4.3- Average concentrations of TSS obtained at inlet and outlet to different OLRs..... | 20 |
| Table 4.4- Average concentrations of VSS obtained at inlet and outlet to different OLRs. | 20 |
| Table 4.5 – Biomass density obtained at different OLRs, from cell 1, cell 2 and cell 3..... | 22 |
| Table 4.6- tCOD averages concentrations and removal rate efficiencies obtained for inlet and outlet at different OLRs..... | 22 |
| Table 4.7- sCOD averages concentrations and removal rate efficiencies obtained for inlet and outlet at different OLRs..... | 23 |
| Table 4.8- COD surface loading rate ($\text{g COD m}^{-2} \text{ d}^{-1}$) at different OLRs. | 24 |
| Table 4.9- Total BOD concentrations and respectively removal efficiencies at OLRs applied.. | 26 |
| Table 4.10- Soluble BOD concentrations and respectively removal efficiencies at OLRs applied. | 26 |
| Table 4.11- BOD surface loading rates ($\text{g BOD m}^{-2} \text{ d}^{-1}$) at different OLRs. | 27 |
| Table 4.12- Ammonia inlet and outlet average concentrations and respectively removal efficiency, at OLRs applied..... | 28 |
| Table 4.13- N-NH_4^+ surface loading rate ($\text{g N-NH}_4^+ \text{ m}^{-2} \text{ d}^{-1}$) at different OLRs..... | 28 |
| Table 4.14- Removal rates obtained at different mixing intensities for Media 1, 2 and 3. | 33 |
| Table 4.15- Summary of the results obtained from three different medias, for sCOD removal, Mass transfer, Boundary layer and removal efficiency..... | 37 |

This page was intentionally left blank

List of Equations

| | |
|---|----|
| Equation 1- Biochemical reaction of organic removal..... | 2 |
| Equation 2- External Mass Transfer coefficient..... | 12 |
| Equation 3- Boundary Layer Thickness..... | 13 |
| Equation 4- Formula for determination of the diffusion coefficient of the oxygen in the biofilm. | 13 |
| Equation 5- Organic loading rate ($\text{g m}^{-2} \text{ day}^{-1}$). | 13 |
| Equation 6- Removal Organic loading rate ($\text{g m}^{-2} \text{ day}^{-1}$). | 13 |
| Equation 7 - Obtainable removal rate ($\text{gCOD m}^{-2} \text{ day}^{-1}$). | 14 |
| Equation 8- Suspended solids concentration). | 14 |
| Equation 9 - Unseeded BOD_5 | 15 |
| Equation 10 - Seeded BOD_5 | 15 |
| Equation 11 - Biomass density calculation. | 16 |
| Equation 12- Biomass concentration calculation. | 16 |

This page was intentionally left blank

List of acronyms

ASP – Activated Suspended Plant

BAF- Biological aerated filters

BOD – Biochemical Oxygen Demand

BOD₅ – 5 days Biochemical Oxygen Demand

COD – Chemical Oxygen Demand

DO – Dissolved Oxygen

EPS- Extracellular polymeric substances

MBBR – Moving Bed Biofilm Reactor

MLSS – Mixed Liquor Suspended solids

MLVSS- Mixed Liquor Volatile Suspended Solids

OCT - Optical Coherence Tomography

OLR- Organic Loading Rate

PST – Primary settling tank

RBC- Rotating Biological Contactors

SAF – Submerged Aerated Filters

TF- Trickling Filters

TSS – Total Suspended solids

VSS – Volatile suspended solids

VVM - Vessel Volume/Minute.

WWTP – Wastewater Treatment

This page was intentionally left blank

1. Introduction

Nowadays wastewater treatment has become an important issue of modern society. Globally, over 80% of all wastewater resulting from municipal, industrial and agricultural activities is returned to the water cycle without being treated. Approximately 30% of all diseases and 40% of deaths around the world are due to polluted water [1].

Wastewater consists of 99.9w/w% water, whereas the remaining 0.1w/w% corresponds to suspended or dissolved material. Despite the latter being a small percentage, this portion has negative impacts in water courses, therefore in human health[2]·[3]. Thus the conventional wastewater treatment processes need to be upgraded or replaced with new and advanced technologies, in order to maximise the efficiency and reduce the costs of the operation [4].

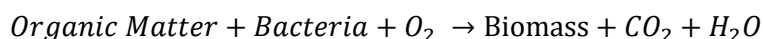
There are different sources of wastewater, such as domestic, industrial, commercial or agricultural activities. It is important to know the source of wastewater to determine the appropriate approach for the treatment process. The principal concern about wastewater treatment is the enrichment of organic matter and nutrients in water courses (phosphorus and nitrogen), nutrients cause several problems, e.g. eutrophication, when discharged to the environment [5].

Wastewater treatment plants (WWTPs) aim to convert wastewater into an effluent that can be discharged to a natural water cycle without contaminating it. [6] In WWTP combinations of physical, biological and chemical methods are used to purify water, which consists of the following steps: preliminary and primary treatment (physical process), secondary treatment (biological process) and tertiary treatment (chemical process) [3].

Preliminary and primary treatment are physical processes used to remove large fractions of inorganic materials. The preliminary (pre-treatment) treatment removes all large materials found in raw wastewater, such as, pieces of wood, cans, rags, plastic packets, etc., to avoid damaging or clogging of pumps and pipes of the treatment plant. This step is usually accomplished by screening and grit removal [7]. The primary treatment allows the removal of settleable and floatable solids, which requires a settling tank, where flow velocity is reduced to achieve hydraulic retention times of between 2 and 4 hours. This step allows the settling of heavier solids to the bottom, forming primary sludge, and floating of lighter solids to the surface [8][9].

Secondary treatment is a biological process which can achieve a 85% of solids removal through flocculation and settling [10]. This step aids to reduce organic matter and nutrients in wastewater [11]. The organic matter remaining, after the primary treatment, is stabilized by biological activity. The active microorganisms in wastewater, such as bacteria (heterotrophic or autotrophic), algae and fungi, use the organic matter as energy or reproduction, through oxidation reactions. This leads to biomass growth and wastewater purification [3]·[7].

Generally, the bacterial growth can be explained by the following simplified Equation 1.1. Biodegradable organic material is biochemically oxidized by heterotrophic bacteria under aerobic conditions resulting in production of carbon dioxide, water, ammonia and new biomass.



Equation 1.1- Biochemical reaction of organic removal.

Nutrients accumulated in wastewater, such ammonia and phosphorus, lead to eutrophication, which has a negative impact on aquatic life. Therefore, accomplishing nutrients removal is a crucial step in biological wastewater treatment. Nitrification process aims to convert ammonia to nitrate using aerobic autotrophic bacteria. [12]. This process can be influenced by several factors, as organic load, dissolved oxygen concentration, $\text{NH}_3\text{-N}$ concentration temperature, pH and alkalinity [13].

After biological treatment, the influent can be submitted to a tertiary (or advanced) treatment. This step, is mostly applied as a combination of primary and secondary treatment to improve the water quality and remove specific wastewater constituents which cannot be removed by secondary treatment [7].

Biological wastewater treatments, are the most common systems used for organic pollutants removal, the reason being that they are economically advantageous as opposed to chemical processes. They can be classified as aerobic or anaerobic systems and suspended growth or attached growth.[3]

Suspended growth systems, are the most common process in wastewater treatment. In this type of system biomass grows in the suspended or dispersed form without any attachment support. Activated sludge processes (ASPs) are based on an aerated tank where suspended microorganisms degrade the organic matter, resulting in dispersed flocs. A settling tank is installed followed by the bioreactor, to settle the secondary sludge and remove it thereafter. [3]

ASPs are used in municipal and industrial wastewater treatment, as they are effective for organic carbon and nutrient removal. [6] However, these processes have several disadvantages, namely, high energy consumption and high capital operating costs.

On the other hand, attached growth systems, have been proven to be reliable for wastewater treatment, since they have more advantages than suspended growth systems. Among many advantages they are known to tolerate variations in hydraulic and pollutant load, having a small footprint and a low operational and maintenance cost. Commonly, they are applied to municipal wastewater treatment. These systems are based on attached biomass growth, i.e. biofilm growth,

where microorganism grow attached to packing material support (e.g. glass, plastic, powdered minerals, fibrous carriers). [4]

Attached growth systems can be classified as fixed (static material support within the reactor) or mobile (material support is kept in suspension inside of the reactor) [14]. The most common processes used in attached growth systems are trickling filters (TF) and rotating biological contactors (RBC) (Fig.1.1). Both are non-submerged fixed biofilm systems. However, over the last few years, new technologies have been developed to improve the performance of attached growth systems. Mobile bed biofilm systems are an example of these recent technologies, such as the moving bed biofilm reactor (MBBR) and submerged aerated filters (SAFs).

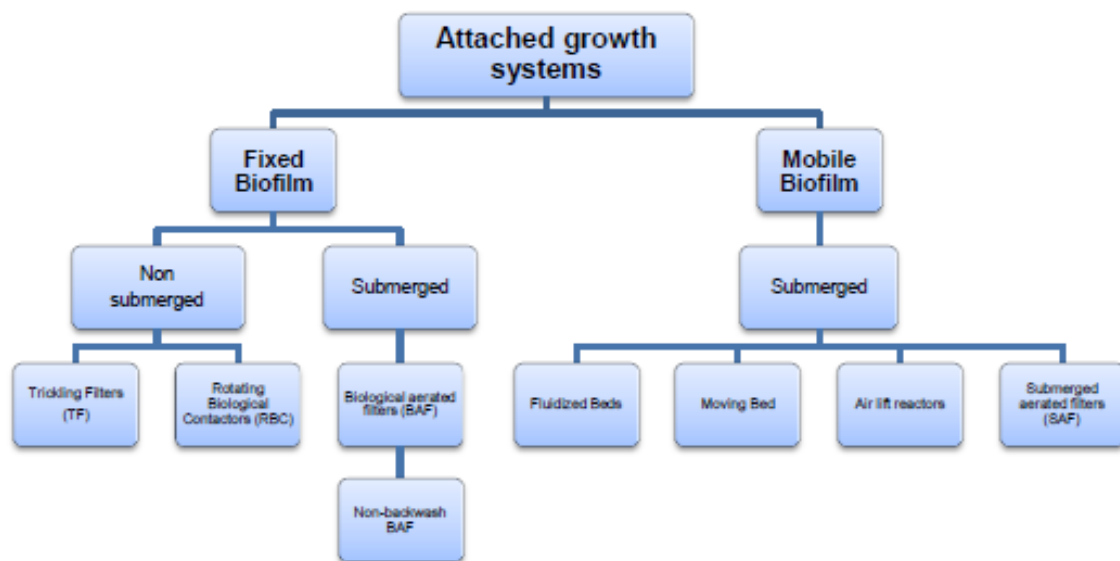


Figure 1.1 - Attached processes for biological wastewater treatment. [11]

MBBR and SAF technology, have been shown to have several advantages over conventional processes, such as improved mass transfer, reduced biofilm diffusion limitations and accelerated biofilm/bulk liquid transfer. This new technology is mostly applied for small communities, but new studies have been developed to enhance the efficiency of reactors, in order to expand the capacity to larger communities of wastewater treatment plants. MBBR and SAFS are often used for organic matter removal, ammonia oxidation and total nitrogen removal, applicable for municipal as well as industrial wastewater treatment [11].

MBBR technology is one of advanced wastewater treatment having advantaged of both attached and suspended growth systems. It is mostly applied for municipal and industrial wastewater treatment in the secondary or tertiary stage [4]. They are designed to treat a wide range of organic loads to provide denitrification and removal of organic matter and ammonia.

MBBR shows many advantages over common wastewater treatment processes, such as holding high biomass attached to the support, high COD loading, strong tolerance to loading impact, relatively smaller reactor and no sludge bulking problem. They can be operated in aerobic or anoxic systems, where mixing can be achieved by aeration, for the first process, and by using mixers for the second. The mixing within the reactor is done to ensure that the plastic carriers are maintained in suspension in order to provide better chances of uniform biofilm growth [13][4].

Several parameters affect MBBR performance such as flow and mixing conditions, filling ratio of media (percentage of reactor volume comprised of media), specific area of carrier media, presence of dissolved oxygen and biofilm development. To achieve uniform growth of biofilm in plastic carriers, it is recommended to provide an ideal mixing intensity, since high turbulence detaches biomass from the media. Furthermore, a biofilm thickness less than 100 μm is preferred to ensure substrate and oxygen penetration. A filling ratio of up to 70% is also recommended to increase reactor efficiency, since higher filling ratios for MBBR can lead to greater collision between media, resulting in microorganism detachment and consequently a decrease in biomass within the reactor. However, lower filling ratios decrease the surface area available to biomass growth [4].

High specific area carriers can support high concentrations of attached biofilm in a small reactor. The biofilm supports should have a specific surface area from 200 - 1200 m^2/m^3 , and a density similar to water. The dissolved oxygen (DO) must be higher than 2 mg L^{-1} for efficient COD and higher than 6 mg L^{-1} for ammonia removal[4]. The biofilm attachment and detachment process, i.e. biofilm development, is influenced by various factors such as adsorption and desorption of microorganisms to the solid surface, biofilm growth, thickness and biofilm adhesion. [4] For the nitrification process (ammonia removal), several studies have demonstrated that organic loading rate (OLR), DO and temperature are parameters that can strongly influence ammonia removal. Medium rate MBBRs can treat 10 to 15 $\text{g COD m}^{-2} \text{d}^{-1}$ and 5 to 10 $\text{g BOD m}^{-2} \text{d}^{-1}$ loads and reach 80-90% of BOD removal.[11]

SAF technology is a submerged attached growth system which has been used as an alternative to ASP over the past few years. It aims to reduce amounts of BOD and ammoniacal nitrogen in settled sludge for wastewater treatment at secondary or tertiary treatment. In SAF technology the biofilm support used has high voidage ($<400 \text{ m}^2/\text{m}^3$), to create a large contact area for biofilm growth [11][15]. SAFs are efficient when low OLRs are applied and can be operated in a range of 3 to 30 $\text{g COD m}^{-2} \text{d}^{-1}$ for domestic wastewater [16]. They can achieve 85% and 65% of COD removal rate at 3 and 30 $\text{g COD m}^{-2} \text{d}^{-1}$, respectively. For nitrification, removal rates of 0.3 to 1.45 $\text{g N-NH}_4^+ \text{m}^{-2} \text{d}^{-1}$ are also achieved for the ranges of OLR mentioned [11].

In MBBR and SAF systems the biofilm has an important role in the wastewater treatment process. The performance of the reactor can be controlled by mechanisms of biofilm development, such as consumption rate and substrate transport through boundary layer between bulk liquid phase and bacteria [16].

Biofilm can be defined as a mixture of active microbial species, inert cells, and extracellular polymeric substances (EPS). The biofilm cells can get their nutrients either from the support material on which they grow attached, or from the bulk liquid [4]. Biofilm development can be classified in five stages: initial attachment, irreversible attachment, EPS formation, maturation and dispersal. Initial attachment starts to occur when microorganisms in wastewater are exposed to a material surface where they can grow attached to the support through the diffusion mechanism [17]. Irreversible attachment corresponds to the stage when attached cells create microcolonies. Once the microorganisms start to grow attached to the support, they start to produce EPSs, a gel-network which keeps bacteria together in biofilm and increases with the age of biofilms [1][18]. In the maturation stage, the biofilm starts to grow in three dimensions. Dispersal is the final step of biofilm development where bacterial cells disperse from biofilms [18]. (Fig.1.2)

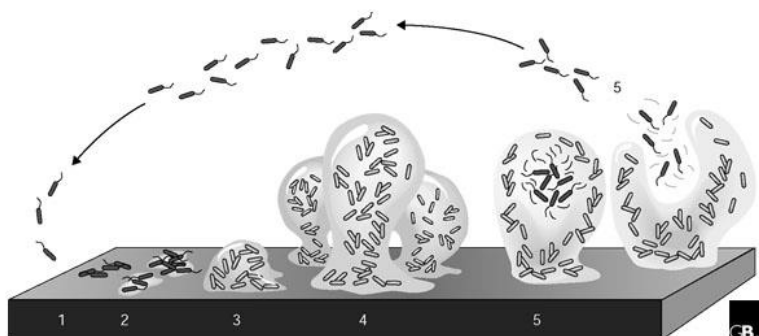


Figure 1.2-Biofilm development stages. Stage 1 Initial attachment, Stage 2- Irreversibly attachment, Stage 3- EPS formation, Stage 4- maturation and Stage 5- dispersal. [19]

In order to ensure that microbial growth occurs, several parameters need to be controlled to improve bacterial activity and the rate of biochemical reactions within the reactor, e.g. nutrients concentration, pH temperature, surface topography, velocity, turbulence, hydrodynamics and EPS production.

Temperatures between 12°C- 25°C and pH around 7 are recommended. Higher temperatures increase biological metabolism and activity in wastewater and increase the organic removal rates. However, the increased metabolism may lead to problems of oxygen limitations [3]. A rough surface is desired for better biofilm attachment to the media, due to the roughness contributing to a larger surface area [18]. Production of EPSs is recommended due to the fact that it helps to aggregate the biofilm cells [1]. Fig. 1.3 shows a schematic representation of a biofilm system.

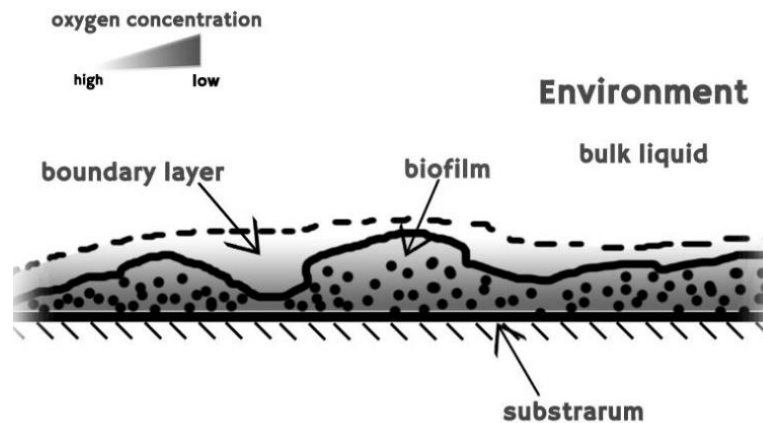


Figure 1.3 – Schematic representation of biofilm structure. [20]

The biofilm structure consists of a liquid phase, gas phase, support surface and the biofilm itself. Between the liquid phase and the biofilm, a stagnant film resulting from mass transfer resistance appears, where the pollutants pass through in order to reach the biofilm (Fig. 1.4). Within the biofilm the substrates are transported by diffusion due the concentration gradient generated by the consumption of the pollutants [16][21]. The external mass transport is affected by the mixing intensity within the reactor. High mixing intensities can increase the mass transfer rate, thereby increasing pollutants removal performance. However, at higher mixing intensities, collisions between the media are also higher, which can lead to biomass detachment [21]. The removal efficiency of the pollutants through the bacteria depends on the thickness of the biofilm. Although biofilm is a hydrated structure, the diffusion of the substrate within the biofilm is lower than the diffusion of the substrate in water, mostly due the presence of microbial cells, EPS or gas bubbles in biofilm. Thus, the consumption rate and substrate transport can be influenced by biofilm thickness, considering that diffusion limitations occur in the deepest regions of the biofilm [21].

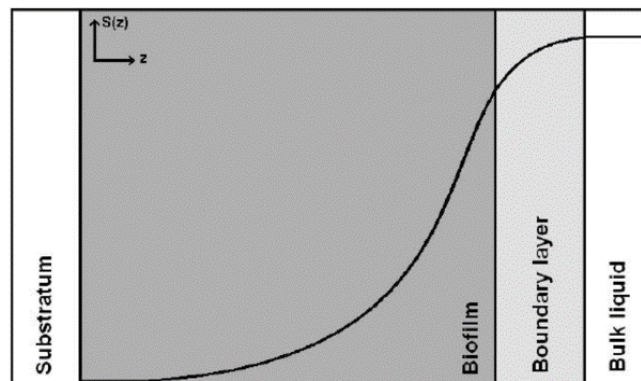


Figure 1.4- Substrate concentration consumption throughout the biofilm thickness at different stages.[22]

2. Objectives

The aim of this work was study the performance of a pilot-plant MBBR/SAF technology containing Biofil plastic media carriers (protected surface area of $112 \text{ m}^2 \text{ m}^{-3}$) for a period of six months. Different municipal wastewater feeding rates were applied to vary organic loads (6, 8, 12 and $16 \text{ g COD m}^{-2} \text{ d}^{-1}$). The efficiency of organic and ammonia removal was investigated to understand what were the maximum loading rate that could be applied.

In parallel, the external mass transfer and the boundary layer thickness of three different media, Biofil, Biomarble and Biopipe (protected surface area of $112 \text{ m}^2 \text{ m}^{-3}$, $220 \text{ m}^2 \text{ m}^{-3}$, $348 \text{ m}^2 \text{ m}^{-3}$) were also investigated.

This page was intentionally left blank

3. Material and Methods

3.1 Media Studied

Three different carrier media were used in this study. Media 1, Media 2 and Media 3 were provided by Warden Biomedia, a carrier media manufacture, situated in Luton, UK (Table 3.1).

Table 3.1 - Media carriers used for the performance study of MBBR/SAF technology.

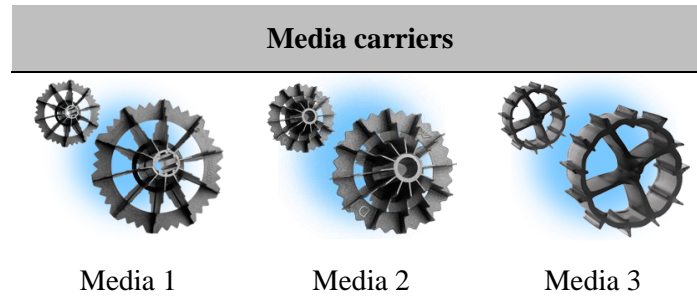


Table 3.2 shows physical properties of each media used in this study. As a common practice in MBBR/SAF, the carrier media protected surface area was used for all calculations, since not all the carrier media surface is used by the biofilm. The densities of the three media used in the case study were 0.97g cm^{-3} .

Table 3.2- Physical properties of studied medias.

| Media | Surface area m^2m^{-3} | Protected surface area m^2m^{-3} | Dimensions Depth: Diameter | Material | Voidage |
|---------|---|--|-------------------------------|---------------------------|---------|
| Media 1 | 135 | 112 | 65:95 | Recycled Polypropylene | 95% |
| Media 2 | 310 | 220 | 46:36 | Recycled Polypropylene | 90% |
| Media 3 | 600 | 348 | 13:21.5 | Recycled Polypropylene | 82,5% |

3.2 Pilot-scale MBBR/SAF technology performance experiments

The performance study of mobile biological attached growth systems was carried out in a MBBR/SAF pilot-scale and operated in continuous mode treating the incoming wastewater from Cranfield University wastewater treatment plant (WWTP) incorporated in Cranfield University campus. Process performance, was evaluated for a period of 6 months (1/03/2017 – 1/09/2017). A MBBR/SAF reactor with a total liquid volume of 1.95m^3 (1.0 width x 1.5 length x 1.30 height) was used in this study. The reactor was filled with Media 1 at 60% of the volume of empty reactor (filling ratio). Media 1, is a spherical media with $135\text{ m}^2\text{ m}^{-3}$ of total surface area and $112\text{ m}^2\text{ m}^{-3}$ of protected surface area, 95 mm of diameter and a voidage of 95%. Aeration was supplied to the reactor by medium bubbles diffusers that were installed at the bottom of the reactor. An additional settling tank was installed to decrease incoming solids. All the particulate matter was removed from the bottom of the settler. After the additional pre-treatment, wastewater was pumped into the reactor for biological treatment. The reactor was designed with three compartments separated by vertical baffles. The inlet was situated at the bottom of the tank, while the outlet was situated at the top for better flow distribution. The experimental set-up for MBBR/SAF is shown in Fig. 3.1 and Fig.3.2.



Figure 3.1- Pilot scale MBBR/SAF reactor used in study case.

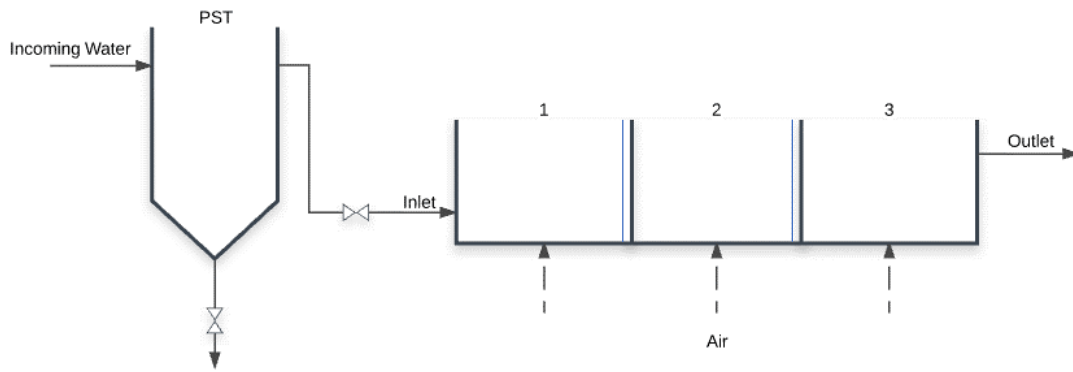


Figure 3.2- Scheme of MBBR/SAF used in this study case.

3.3 Organic loading rates increase

The MBBR/SAF process was evaluated by increasing the organic loading rate (OLR). The OLRs applied were 6, 8, 12 and 16 g COD m⁻² d⁻¹ in order to study the performance of the reactor.

3.4 External mass transfer experiments

Regarding external mass transfer experiments, the experimental design for the external mass transfer experiments was as described by Bruno L Nogueira 2015, was used as methodology for the experimental investigation. Appendix I describes the calculations used in the methodology mentioned, for determination of external mass transfer coefficient and boundary layer thickness.

All experiments were done in duplicate in order to minimize the errors of standard deviation of each trial. The experiments to determine the external mass transfer were carried out in a MBBR/SAF lab-scale reactor, operated in continuous mode for the three media (Table 2). The volume of the reactor was 36L and operated under a hydraulic retention time of 2h with 60% fill ratio for each media. (Fig. 3.3)



Figure 3.3- Lab-scale MBBR/SAF used in this study case.

The experiments carried out for Media 1, Media 2 and Media 3, were operated using the wastewater coming from Cranfield WWTP. The lab reactor was operated continuously during 2 to 3 weeks before starting the experiments to ensure biofilm growth. Once the biofilm was formed, the feeding was stopped, and the biomass aerated until complete organic removal occurred.

During the experiments, DO was kept at 2.5-3.5 mg L⁻¹ by controlling aeration and nitrogen flow rates, pH was kept around 7.4 using a HCl solution and the temperature was kept constant at 20°C using heater controllers.

To study substrate consumption by the biomass, an excess of sodium acetate (NaHCO₃) was added. Each trial lasted for one hour with a sampling time of 15min. Collected samples were filtered for soluble COD measurement to determine the substrate concentration consumption. Tests were carried out at different mixing intensities, by controlling the increasing air flow rate. Mixing intensities were increased until no effect on removal rate of the COD was observed, as shown in Fig. 3.4.

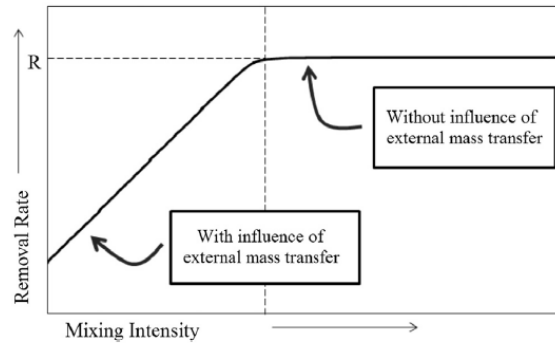


Figure 3.4- Schematic variation of the substrate removal rate. The mixing intensity is increased until no effects of external mass transfer coefficient is observed in removal rate . [16]

The mass transfer coefficient and the boundary layer thickness were obtained throughout Equation 3.1 and 3.2. The oxygen diffusion coefficient is given by Equation 3.3.

$$k_{O_2} = \frac{V_{bulk}}{A} * \frac{r^{exp} * R^2}{R^2 - r^{exp2}} * \frac{\gamma_{O_2}}{S_{O_2}^{bulk}}$$

Equation 3.1- External Mass Transfer coefficient.

Where,

V_{bulk} is the volume of liquid inside m³;

A is the total surface area of the carriers within the reactor m²/m³;

$\gamma_{\frac{O_2}{substrate}}$ is the stoichiometric factor and is the ratio of the oxygen to the substrate uptake;

R is the volumetric removal rate where external mass is neglected $\text{mg L}^{-1} \text{h}^{-1}$;

$$\delta = \frac{D_{O_2}^{water}}{k_{O_2}}$$

Equation 3.2- Boundary Layer Thickness.

Where,

δ is the boundary layer thickness μm ;

$D_{O_2}^{water}$ is the oxygen diffusivity in water $\text{m}^2 \text{h}^{-1}$.

$$R \gamma_{\frac{O_2}{substrate}} \frac{V_{bulk}}{A} = \sqrt{2D_{O_2}^{biof} q_{O_2,max} * X} * \sqrt{S_{O_2}^{bulk}}$$

Equation 3.3- Formula for determination of the diffusion coefficient of the oxygen in the biofilm.

Where,

$q_{O_2,max}$ is the maximum substrate specific conversion rate $\text{g g}^{-1} \text{h}^{-1}$;

$D_{O_2}^{biof}$ is the oxygen diffusivity in the biofilm $\text{m}^2 \text{h}^{-1}$;

$S_{O_2}^{bulk}$ is the liquid phase concentration mg L^{-1} ;

X is the biomass density g L^{-1} .

3.5 Analytical methods

Important process parameters for SAF/MBBR are the organic loading rate (OLR) and the removal organic loading rate (ROLR), that can be expressed by the daily pollutant load applied to and removed from a volume of media with a known specific surface area. (Equation 3.4 and 3.5)

$$OLR = \frac{[COD_i] * flow}{\text{specific surface area} * \text{Fill Ratio} * V_r}$$

Equation 3.4- Organic loading rate ($\text{g m}^{-2} \text{d}^{-1}$).

$$ROLR = \frac{[COD_i - COD_f] * flow}{\text{specific surface area} * \text{Fill Ratio} * V_r}$$

Equation 3.5- Removal Organic loading rate ($\text{g m}^{-2} \text{d}^{-1}$).

According to Odegaard et al., 1994 and Odegaard et al., 2000 an “obtainable removal rate” should be used to calculate COD removals without the influence of the performance of the clarifier and the solids produced by biomass detached from the carrier media. The calculations are based on the total COD inlet and soluble COD at the outlet. (Equation 3.6)

$$\text{Obtainable removal rate} = \frac{[tCOD_{in} - sCOD_{out}] * flow}{\text{specific surface area} * \text{Fill Ratio} * V_r}$$

Equation 3.6 - Obtainable removal rate (gCOD m⁻² d⁻¹).

To measure the performance of the pilot-scale reactor, samples were taken from the influent and final effluent of the reactor. Total and volatile suspended solids (TSS and VSS), total and soluble chemical oxygen demand (tCOD and sCOD), total and soluble biochemical oxygen demand (tBOD and sBOD) and ammonia removal were measured three times a week. Biofilm was collected from the reactor twice a week to measure attached biomass growth and extracellular polymeric substances (EPS). pH, DO and temperature were measured daily.

3.5.1 Dissolved oxygen (DO), pH and temperature

HQ40d Digital Multi-Parameter Meters from Hach® were used to measure the dissolved oxygen concentration and pH in the reactors during the experiments.

3.5.2 Total and volatile suspended solids (TSS and VSS)

The procedure described here follows Standard Methods 208 E (2005), 2540D and EPA (1983) Method 160.2. Measurement of wastewater samples were accomplished by using Glass Microfibre filters GF/A WHATMAN™. A volume of 100 ml of wastewater was filtered with glass fibre pads. Then the pads were pre-heated at 150 °C overnight to ensure the removal of any remaining water, and left into a desiccator to cool to room temperature for TSS quantification. For VSS measurement, the procedure was similar, the pads were heated at 550°C for 2h and then left into a desiccator until cool down to room temperature. Once they have reached the room temperature, the pads were weighted with a digital balance[25]. To calculate TSS and VSS value Equation 3.7 was applied.

$$SS = \frac{W_{post} - W_{pre}}{V} * 1000$$

Equation 3.7- Suspended solids concentration).

Where,

SS- Suspended solid (mg L⁻¹)

W_{post} – Filtered weight (g)

W_{pre} - Filer wright (g)

V- sample volume (ml)

3.5.3 Total and soluble Chemical Oxygen Demand (tCOD and sCOD)

For COD measurements, MERCK COD Cell Tests were used. A range of 25-1500 mg L⁻¹ and 10-150 mg L⁻¹ was used for total and soluble COD.

3.5.4 Total and soluble Biochemical oxygen demand (tBOD and sBOD)

BOD test is the standard method used for indirect measurement of amount of organic pollution, that can be oxidized biologically in wastewater sample. This test indicates the amount of dissolved oxygen that is consumed by bacteria in a 5 days period of incubation. High values of BOD can indicate high amounts of pollution in wastewater sample [26].

The total and soluble BOD were estimated by the dilution method, mentioned by U.S. EPA, Method 5210B in the Standard Methods for the Examination of Water and Wastewater. For BOD₅ measurements, DO concentration was measured before and after the incubation period. Five duplicate samples of wastewater with specific dilution factors, including the blank solution, all containing a volume of 500ml, were used in the tBOD and sBOD determination. The blank solution was used to confirm the quality of the dilution water that was used to dilute the samples. The dilution factors applied were: 10:500, 25:500, 50:500 and 100:500. The first two factors used were for tBOD and the two second ones for sBOD. The dilution water used in this test, was prepared by adding seed microorganisms and leaving them aerated for at least 2 hours, to ensure that the water was saturated with oxygen. After the preparation of the solutions and the reading of the initial DO, the samples were kept in a dark room at 20°C to prevent DO production via photosynthesis, for 5 days. The BOD₅ initial and final concentration were given by Equations 3.8 and 3.9, respectively.

$$BOD_5 = \frac{D_0 - D_5}{P}$$

Equation 3.8 - Unseeded BOD₅.

$$BOD_5 = \frac{(D_0 - D_5) - (B_0 - B_5) * f}{P}$$

Equation 3.9 - Seeded BOD₅.

Where,

D_0 - Dissolved oxygen of dilution of the prepared solution, mg L⁻¹

D_5 - Dissolved oxygen of diluted solution after 5 days of incubation, mg L⁻¹

P – Decimal dilution factor

B_0 - Dissolved oxygen of blank solution, mg L⁻¹

B_5 - Dissolved oxygen of blank solution after 5 days of incubation, mg L⁻¹

f - Seed volume ratio.

3.5.5 Ammonia

For Ammonia measurements, MERCK Ammonia Cell Test cell test kit was used, ranged from 4.0 – 80 mg L⁻¹.

3.5.6 Attached biomass growth

The measurements of the total solids on the attached biomass were conducted by collecting 5 media of each cell and pre-heating at 105°C overnight. After the media were left to cool until room temperature was reached, they were weighed using an analytical balance. Afterwards, they were cleaned, dried and weighed again. The biomass densities and concentrations were calculated using Equation 3.10 and 3.11 respectively.

$$X = \frac{W_{biomass} - W_{clean}}{TSA}$$

Equation 3.10 - Biomass density calculation.

Where,

X - Biomass density, g m⁻²

$W_{biomass}$ - Media weight with biomass, g

W_{clean} - Clean media, g

TSA - Total surface area of media, m² m⁻³

$$C_{biom} = TS * Fill\ ratio * \frac{Total\ number\ of\ media}{Vr}$$

Equation 3.11- Biomass concentration calculation.

Where,

C_{biom} – Biomass concentration, gTS m⁻¹

TS – Total solids, g

V_r - Volume of the reactor, m³

3.5.7 Extracellular Polymeric Substances (EPS)

EPS are cell aggregates with a complex high-molecular-weight mixture of polymers, generated during biofilm development. In this study, only total EPS were measured, the biofilm attached to the carriers was manually scraped in 250 ml of DI water. It was measured 50 ml of the well mixed biomass and added to 250 ml of water. Afterwards, the sample was concentrated by centrifuge at 5000 rpm during 10 min. Proteins (PN) were determined by using the Lowry method modified by Frolund and Carbohydrates (PS) were determined by Dubois, using phenol sulfuric acid (Nielsen and Jahn, 1999). All the experiments were carried out in triplicate, twice to three times a week for all three reactor cells. The EPS concentration was then expressed as the specific weight expressed as mgPN/gMLVSS and mgPS/gMLVSS.

3.5.8 Optical coherence tomography (OCT)

The OCT was used in this work to capture three-dimensional images of the attached biofilm, to measure of biofilm thickness (Appendix V).

This page was intentionally left blank

4. Results and Discussion

4.1 SAF performance study for Media 1

The average composition of incoming pre-settled wastewater is shown in Table 4.1. The experimental work was carried in a timeframe of six months.

Table 4.1- Influent wastewater characterization (after pre-treatment within six months timeframe).

| Wastewater | Unit | From 1/03/2017 to 1/09/2017 |
|-------------------|------|--------------------------------|
| DO | mg/L | 3.99 ± 0.86 |
| Temperature | °C | 20.8 ± 2.78 |
| pH | - | 7.7 ± 0.15 |
| Total COD | mg/L | 296.74 ± 104.16 |
| Soluble COD | mg/L | 61.62 ± 15.37 |
| BOD ₅ | mg/L | 124.65 ± 37.82 |
| sBOD ₅ | mg/L | 15.17 ± 7.35 |
| Ammonia | mg/L | 30.65 ± 6.32 |

Throughout this experiment, DO, temperature and pH were monitored daily for cell 1, cell 2 and cell 3 of the reactor and, also for the inlet and outlet. In Appendix II the evaluation of these parameters within a six-month timeframe is shown at the different OLRs applied. It was observed that pH values of inlet and outlet remained within a range of 7-8. The temperatures for the three compartments of the reactor varied within a range of 18°C to 25°C.

The DO values inside of the reactor were controlled for each cell and kept within a range of 4 ± 0.86 mg L⁻¹ for the first cell, 4.68 ± 1.0 mg L⁻¹ for the second cell and 5.45 ± 0.99 mg L⁻¹ for the third cell. In the third cell, higher values of DO were achieved to enhance the nitrification process.

The air flow was increased as organic loading rates were increased in order to keep the DO concentration within the mentioned range.

For the first cell, at 6 g m⁻² d⁻¹ the air flow rate applied initially was 70 L min⁻¹. The latter was increased until 140 L min⁻¹ for the highest load, i.e. 16 g m⁻² d⁻¹. Table 4.2 summarizes the flow rate conditions and hydraulic retention times (HRTs) for the organic loads applied. For this study, the flow rate was increased from 2.71 to 3.6, 5.43 and 7.25 m³ d⁻¹ and the respective HRTs calculated were 17.7, 13.3, 8.8 and 6.6 h.

Table 4.2- OLRs, flow rates conditions and HRT applied in MBBR/SAF.

| OLR (g m ⁻² d ⁻¹) | Air flow rate (L min ⁻¹) | | | Flow rate (m ³ d ⁻¹) | HRT (h) |
|---|--------------------------------------|--------|--------|--|------------|
| | Cell 1 | Cell 2 | Cell 3 | | |
| 6 | 70 | 50 | 50 | 2.71 | 17.7 |
| 8 | 80 | 50 | 50 | 3.62 | 13.3 |
| 12 | 110 | 65 | 60 | 5.43 | 8.8 |
| 16 | 140 | 60 | 60 | 7.25 | 6.6 |

4.1.1 Solids removal

The inlet and outlet concentration of total solids suspended (TSS) and volatile solids suspended (VSS) at different OLRs, are shown in Table 4.3 and 4.4.

An average removal efficiency for TSS and VSS of 40% were observed for average OLR applied. The inlet concentrations obtained from TSS and VSS were 202.39, 163.81, 160.44, 134.58 mg L⁻¹ and 182.26, 156.34, 141.38 and 125.92 mg L⁻¹, respectively.

The outlet concentrations obtained from TSS and VSS were 98.17, 91.78, 83.06, 82.33 mg L⁻¹ and 90.67, 93.53, 82.06, 78.33 mg L⁻¹, respectively for the organic loads applied.

Table 4.3- Average concentrations of TSS obtained at inlet and outlet to different OLRs.

| OLR (g m ⁻² d ⁻¹) | TSS mg L ⁻¹ | | Removal TSS |
|---|------------------------|---------------|----------------|
| | In | Out | |
| 6 | 202.39 ± 54.9 | 98.17 ± 33.85 | 49 ± 15.7 % |
| 8 | 163.81 ± 47.64 | 91.78 ± 43.85 | 43 ± 22.8 % |
| 12 | 160.44 ± 54.50 | 83.06 ± 40.52 | 47 ± 18.0 % |
| 16 | 134.58 ± 30.53 | 82.33 ± 56.19 | 39 ± 24.8 % |

Table 4.4- Average concentrations of VSS obtained at inlet and outlet to different OLRs.

| OLR (g m ⁻² d ⁻¹) | VSS mg L ⁻¹ | | Removal VSS |
|---|------------------------|--------------|----------------|
| | In | Out | |
| 6 | 182.26 ± 50.35 | 90.67 ± 29.0 | 48 ± 15.4 % |
| 8 | 156.34 ± 53.53 | 93.53 ± 34.0 | 38 ± 16.6 % |
| 12 | 141.38 ± 46.84 | 82.06 ± 33.0 | 41 ± 16.2 % |
| 16 | 125.92 ± 28.30 | 78.33 ± 49.3 | 37 ± 21.7 % |

It was observed that average removal efficiencies for TSS and VSS were similar for all the different organic loading rate applied, ranging from 49% to 39% and 48% to 37%, respectively.

One of the reasons connected to the lower removal could be because the reactor worked without recirculation of sludge, with a low HRT and due the absence of a secondary settling tank. By considering these low quantities, it was possible to assume a negligible effect of suspended biomass on COD removal performance.[27]

4.1.2 Biomass Growth

Biomass density growth was also monitored to study MBBR/SAF performance. It was observed that the biomass density of the first and second cell increased in response to the organic load increase. (Fig.4.1)

At organic load of $6 \text{ g m}^{-2} \text{ d}^{-1}$ (stage 1) the biomass densities achieved for Media 1 and Media 2 were 14.88 and 8.49 gTS m^{-2} respectively. In the same way, for $8 \text{ g m}^{-2} \text{ d}^{-1}$ (stage 2) were 7.76 and 7.76 gTS m^{-2} respectively, for $12 \text{ g m}^{-2} \text{ d}^{-1}$ (stage 3) were 28.35 and 23.40 gTS m^{-2} respectively, and finally, for $16 \text{ g m}^{-2} \text{ d}^{-1}$ were 36.08 and 26.08 gTS m^{-2} , respectively.

The attached biomass in the third cell was lower compared to the previous first and second cell. At the organic loads applied, for 1st, 2nd and 3rd cell the average values obtained were 5.06 , 7.76 , 5.17 , and 3.69 gTS m^{-2} at organic loads of 6 , 8 , 12 and $16 \text{ g m}^{-2} \text{ d}^{-1}$.

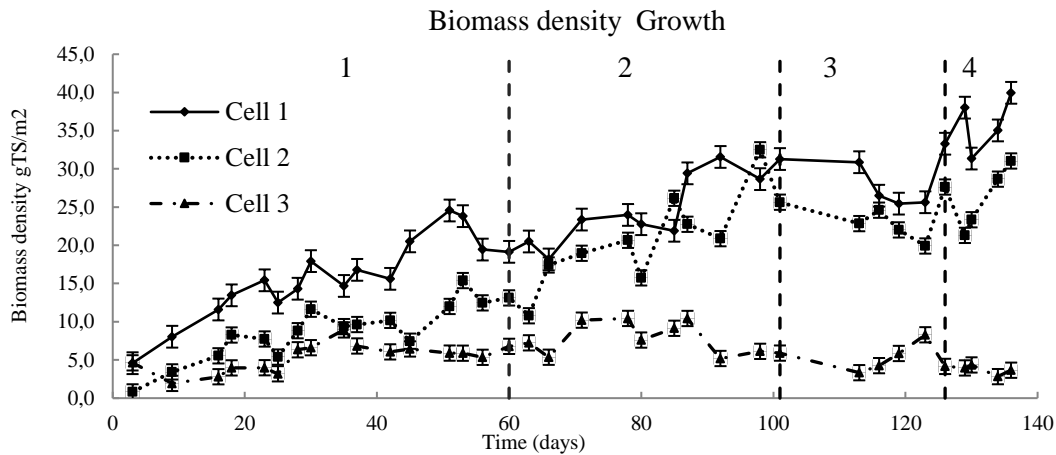


Figure 4.1- Biomass density growth variation obtained from cell 1, cell 2 and cell 3 at different OLRs applied. Stage 1 – day 0 to 60 Stage 2 – day 61 to 101, Stage 3- day 102 to 126 and Stage 4- day 127 to 136.

Table 4.5 shows the average biomass density achieved for each cell at different organic loads.

The 1st and 2nd cell showed that biomass density increased as organic loading increased. This suggests that the attached biofilm, at higher OLRs, was still able to consume the substrate in wastewater.

On the other hand, the 3rd cell of the reactor showed that lower densities were achieved during the experiment, meaning that the majority of pollutants were consumed by bacteria in 1st and 2nd cell, enhancing organic matter removal than nitrification.

Table 4.5 shows the average biomass density achieved for each cell at different organic loads.

Table 4.5 – Biomass density obtained at different OLRs, from cell 1, cell 2 and cell 3.

| OLR (g m ⁻² d ⁻¹) | cell 1 gTS/m ² | cell 2 gTS/m ² | cell 3 gTS/m ² |
|--|---------------------------|---------------------------|---------------------------|
| 6 | 14.88 ± 6.28 | 8.49 ± 3.9 | 5.06 ± 2.10 |
| 8 | 25.16 ± 4.48 | 21.14 ± 5.76 | 7.76 ± 2.02 |
| 12 | 28.35 ± 3.53 | 23.40 ± 2.90 | 5.17 ± 1.96 |
| 16 | 36.08 ± 33.74 | 26.08 ± 4.52 | 3.69 ± 0.65 |

4.1.3 Organic matter removal

The removal efficiencies of soluble and total COD (tCOD and sCOD) at different OLRs are shown in Table 4.6 and 4.7, respectively.

The average removal efficiency for tCOD at lowest OLR, i.e. 6 g m⁻² d⁻¹ (stage 1), was 53 % for an inlet concentration of 317 mg L⁻¹ and for an outlet concentration of 147 mg L⁻¹. At 8,10 and 13 g m⁻² d⁻¹ organic loads (stage 2,3 and 4), the average removal efficiencies obtained were 50%, 55%, 59% respectively, for an inlet concentration of 315, 227 and 236 mg L⁻¹ and outlet of 158, 99, and 113 mg L⁻¹.

Table 4.6- tCOD averages concentrations and removal rate efficiencies obtained for inlet and outlet at different OLRs.

| OLR (g m ⁻² d ⁻¹) | tCOD mg L ⁻¹ | | Removal |
|---|-------------------------|-------------|-----------|
| | In | Out | |
| 6 | 317 ± 104.5 | 147 ± 84.13 | 51 ± 20 % |
| 8 | 315 ± 82.52 | 158 ± 84.66 | 50 ± 20% |
| 12 | 227 ± 55.23 | 99 ± 98.88 | 55 ± 20% |
| 16 | 236 ± 58.60 | 113 ± 73.34 | 59 ± 14% |

Table 4.7- sCOD averages concentrations and removal rate efficiencies obtained for inlet and outlet at different OLRs.

| OLR (g m ⁻² d ⁻¹) | sCOD mg L ⁻¹ | | Removal |
|---|-------------------------|------------|----------|
| | In | Out | |
| 6 | 60 ± 11.15 | 40 ± 9.05 | 41 ± 14% |
| 8 | 71 ± 15.87 | 31 ± 13.79 | 53 ± 10% |
| 12 | 58 ± 18.87 | 35 ± 6.84 | 38 ± 11% |
| 16 | 53 ± 10.66 | 32 ± 5.32 | 38 ± 14% |

In the same way for sCOD removal, the average removal efficiency at lowest OLR, i.e. 6 g m⁻² d⁻¹ was 41% for an inlet concentration of 60 mg L⁻¹ and outlet of 40 mg L⁻¹. At 8, 10 and 13 g m⁻² d⁻¹ organic loads, the average removal efficiencies were 53%, 38%, 38% respectively, for an inlet concentration of 71, 58 and 53 mg L⁻¹ and an outlet concentration of 31, 35, 32 mg L⁻¹.

It was noticed, that at organic loads of 6 g m⁻² d⁻¹ and 8 g m⁻² d⁻¹ the removal efficiencies for tCOD obtained were lower than for the removals obtained from loadings of 12 g m⁻² d⁻¹ and 16 g m⁻² d⁻¹. The inlet and outlet concentrations for total and soluble COD in function of time are represented in Appendix III.

Despite the increase in OLRs, was achieved more than 50% of tCOD removal, at highest OLR applied (16 g m⁻² d⁻¹). Higher efficiencies were obtained for organic loads of 12 g m⁻² d⁻¹.

The surface COD loading rates during the entire operation of MBBR/SAF as a function of time is shown in Fig.4.2. For Stage 1, the average loads obtained for tCOD and sCOD were 5.2 and 1.11 gCOD m⁻² d⁻¹, for stage 2 were 8.5 and 1.92 gCOD m⁻² d⁻¹, respectively, for stage 3 were 9.2 and 2.35 gCOD m⁻² d⁻¹, respectively, and for stage 4 were 12.7 g COD m⁻² d⁻¹ and 2.9 gCOD m⁻² d⁻¹, respectively.

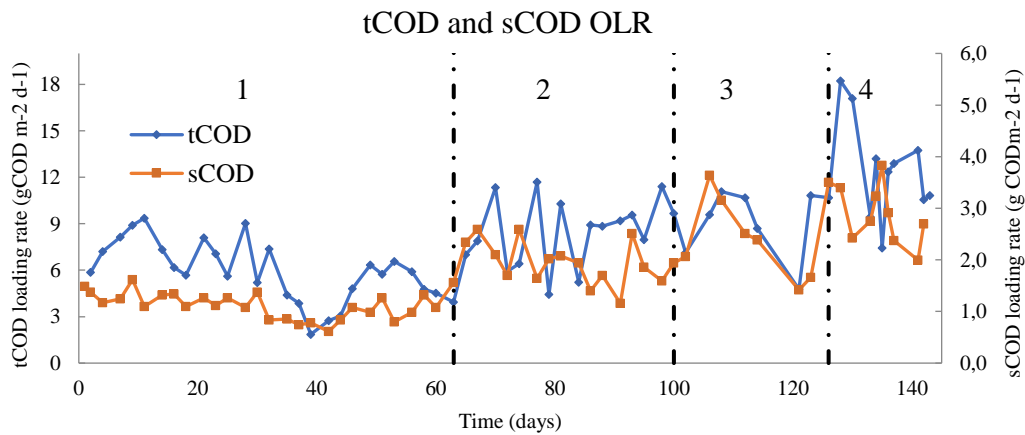


Figure 4.2- Removal OLR of sCOD and tCOD (gCOD m⁻² d⁻¹) versus time (days). Stage 1 – day0 to 63, stage 2 – day 64 to100, stage 3- day 101 to 126 and stage 4- day 127 to 140.

Table 4.8- COD surface loading rate (g COD m⁻² d⁻¹) at different OLRs.

| OLR (g m ⁻² d ⁻¹) | OLR (gCOD m ⁻² d ⁻¹) | |
|---|---|------------|
| | tCOD | sCOD |
| 6 | 5.2 ± 1.8 | 1.11 ± 0.2 |
| 8 | 8.5 ± 2.2 | 1.92 ± 0.4 |
| 12 | 9.2 ± 2.2 | 2.35 ± 0.8 |
| 16 | 12.7 ± 3.2 | 2.87 ± 0.5 |

At total COD loads of 5.2, 8.5, 9.2 and 12.7 gCOD m⁻² d⁻¹, the removal rates achieved were ranging from 2.7 ± 1.6, 4.2 ± 1.9, 5.2 ± 2.7 and 6.6 ± 2.7 gCOD m⁻² d⁻¹, respectively. In the same way, at sCOD loads of 1.11, 1.92, 2.35 and 2.87 the removal rates obtained were ranging from 0.4 ± 0.2, 1.1 ± 0.4, 0.9 ± 0.6 and 1.2 ± 0.5 gCOD m⁻² d⁻¹. (Table 4.8)

It was noted that at stage 4, the dissolved oxygen was ranging from 60 - 140 mg L⁻¹.

Relating HRT with COD removal, it was observed that for an organic load of 12 g m⁻² d⁻¹ (i.e. surface load of 5.2 g tCOD m⁻² d⁻¹) where the highest COD removal efficiency were achieved, HRT was 8.8 h⁻¹, and the flow rate was 5.43 m³ d⁻¹. An average of removal efficiency of 38% of total COD was achieved at the HRT the mentioned. According to Siciliano et al. 2015 [28], the increaisng of HRT can enhance the organic matter removal yields close to 95% (when achieved total COD organic loads of 6 .65 g m⁻² d⁻¹ and HRT of 12 h⁻¹).

The obtainable removal rate for COD is represented in Fig. 4.3 as function of total COD organic loading rate, where the bisector line represents 100% removal efficiency. The obtainable removal rate shows the removal rate of organic matter if all particles (larger than 1 µm) were removed in a downstream separation step. [27]

It was shown that at total COD organic loads the average obtainable removal rates obtained from COD were 4.6 ± 1.7, 7.6 ± 2.2, 7.8 ± 2.2 and 11 ± 3.1 g (tCOD in- sCOD out) m⁻² d⁻¹.

It was noted that a plateau at higher removal rates was starting to reach, meaning that the efficiency of the reactor decreases at loading rates higher than 16 g m⁻² d⁻¹.

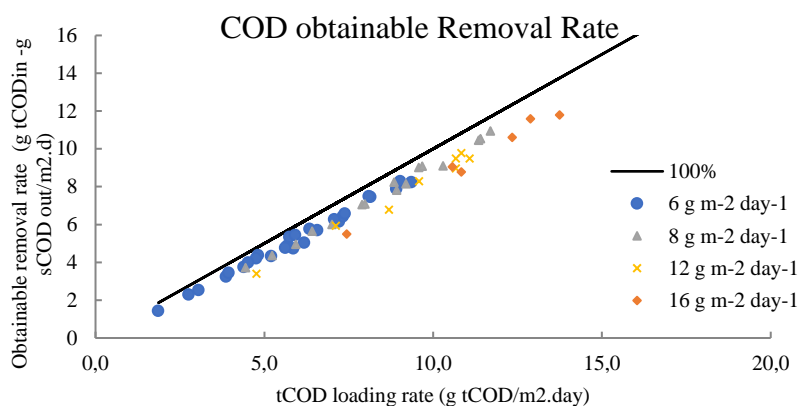


Figure 4.3- tCOD lading rate ($\text{g tCOD m}^{-2} \text{d}^{-1}$) vesus obtainable removal rate ($[\text{g tCODin} - \text{g sCOD out}] \text{m}^{-2} \text{d}^{-1}$)

Many studies have been investigating the overall performance of MBBR. The studies demonstrated that systems can be efficient at higher OLRs studied in present work. According to Aygun et al. 2008[29], a range of OLR between $5.0 - 96.0 \text{ g m}^{-2} \text{d}^{-1}$, could have a total COD removal efficiency ranging from 42.5% - 94.6%. However, according to obtained results in this experimental work, was observed that the COD removal efficiencies were ranging from 53% to 59% for total COD and were ranging from 41% to 38% for soluble COD. The discrepancy of values founded, can be due the absence of secondary settling tank.

The biomass density from 1st and 2nd cell of the reactor was increasing as organic load was increased. The compartments were designed to carried out organic removal, as mentioned before. As biomass density was increasing, it was expected that as organic loads were increased, COD removal rates were also expected to increase. However, an increasing on soluble COD removal rates were observed until an organic load of $12 \text{ g m}^{-2} \text{d}^{-1}$ was reached. Although at organic loads up to $16 \text{ g m}^{-2} \text{d}^{-1}$, the biomass density was still increasing, and the soluble COD removal started to decrease, suggesting the biofilm development was not related with removal of pollutants in wastewater.

The average concentrations of removal rate efficiencies obtained for total and soluble BOD are represented in Table 4.9 and 4.10. At lowest OLR the total and soluble BOD average concentrations for the inlet were 139 and 13 mg L^{-1} , respectively and for the outlet were 47 and 2.8 mg L^{-1} , respectively.

For the remaining organic loads applied, concentrations of 113 , 108 and 108 mg L^{-1} were achieved for total BOD at the inlet and, 56 , 41 and 92 mg L^{-1} for total BOD at outlet. in the same order, soluble BOD at inlet and outlet was 18 , 15 , 20 mg L^{-1} and 22 , 1.1 ad 3.5 mg L^{-1} , respectively. Higher efficiency removal rates were obtained at OLR of $12 \text{ g BOD}_5 \text{ m}^{-2} \text{d}^{-1}$, with 61% and 92% removals, for total and soluble BOD, respectively.

Table 4.9- Total BOD concentrations and respectively removal efficiencies at OLRs applied.

| OLR (g m ⁻² d ⁻¹) | tBOD mg L ⁻¹ | | Removal tBOD |
|---|-------------------------|------------|-----------------|
| | In | Out | |
| 6 | 139 ± 46.93 | 47 ± 28.86 | 65 ± 15 % |
| 8 | 113 ± 18.25 | 56 ± 22.9 | 52 ± 16 % |
| 12 | 108 ± 22.21 | 41 ± 10.2 | 61 ± 13 % |
| 16 | 108 ± 12.31 | 92 ± 7.43 | 15 ± 2.9 % |

Table 4.10- Soluble BOD concentrations and respectively removal efficiencies at OLRs applied.

| OLR (g m ⁻² d ⁻¹) | sBOD mg L ⁻¹ | | Removal sBOD |
|---|-------------------------|------------|-----------------|
| | In | Out | |
| 6 | 13 ± 8.12 | 2.8 ± 1.8 | 74 ± 20 % |
| 8 | 18 ± 6.80 | 2.2 ± 0.63 | 87 ± 5 % |
| 12 | 15 ± 5.19 | 1.1 ± 0.33 | 92 ± 4 % |
| 16 | 20 ± 4.36 | 3.5 ± 0.39 | 82 ± 2 % |

The evaluated inlet and outlet concentrations for total and soluble BOD are represented in Appendix III, as function of time. Soluble BOD concentrations, for inlet and outlet showed higher variations than total BOD. According to obtained results, removal rates efficiency at OLRs higher than 12 g BOD₅ m⁻² d⁻¹ started to decrease.

For the organic load where, maximum removal efficiency was obtained, soluble and total BOD efficiencies were ranging from 61% - 65 % and ranging from 74% - 82%, respectively.

According to literature, soluble BOD removal can be achieved within a range of 75% – 95% at OLRs ranging from 1- 60 g BOD₅ m⁻² d⁻² applied [11].

It was obtained surface organic loads of 2.58, 3.06, 4.35 and 5.84 g BOD m⁻² d⁻¹ for total BOD at 6, 8, 12 and 16 g m⁻² d⁻¹ organic loads and 0.24, 0.48, 0.61, and 1.07 g BOD m⁻² d⁻¹ for soluble BOD at the same organic loads. (Table 4.11)

Table 4.11- BOD surface loading rates ($\text{g BOD m}^{-2} \text{d}^{-1}$) at different OLRs.

| OLR ($\text{g m}^{-2} \text{d}^{-1}$) | OLR ($\text{gBOD m}^{-2} \text{d}^{-1}$) | |
|--|--|-----------------|
| | tBOD | sBOD |
| 6 | 2.58 ± 0.87 | 0.24 ± 0.15 |
| 8 | 3.06 ± 0.49 | 0.48 ± 0.18 |
| 10 | 4.35 ± 0.89 | 0.61 ± 0.20 |
| 13 | 5.84 ± 0.66 | 1.07 ± 0.23 |

The removal rates obtained for total and soluble BOD evaluated over time are shown in Fig. 4.4. For total BOD, the average removal rates obtained from stage1, 2, 3 and 4 were 1.70 ± 0.74 , 1.56 ± 0.49 , 2.71 ± 0.98 and 0.89 ± 0.27 $\text{g BOD m}^{-2} \text{d}^{-1}$. In the same way, for sBOD the average removal rates obtained were 0.19 ± 0.13 , 0.42 ± 0.19 , 0.57 ± 0.21 and 0.87 ± 0.22 $\text{g BOD m}^{-2} \text{d}^{-1}$.

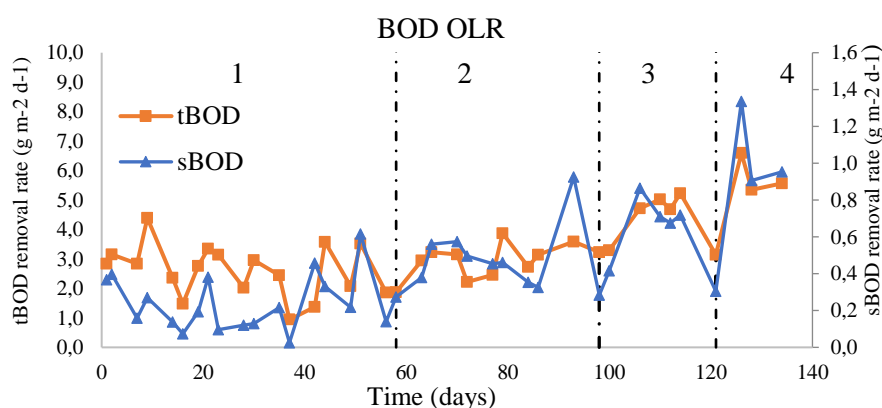


Figure 4.4- tBOD and sBOD removal ($\text{gBOD m}^{-2} \text{d}^{-1}$) versus time (days) for different OLRs applied. Stage 1 – day 0 to 58, stage 2 – day 59 to 98, stage 3- day 99 to 121 and stage 4- day 122 to 134.

4.1.4 Ammonia removal

Temperature and pH were kept within a range of 19-25 °C and 7.5-8, respectively. It was noted that dissolved oxygen concentration in the third cell (5.45 ± 0.99 mg L^{-1}) was higher than DO obtained from 1st and 2nd cell of the reactor. Higher DO values are required for enhance the nitrification process.

The average ammonium removal efficiencies obtained were 73%, 65%, 65% and 42% at organic loads of 6, 8, 12, and 16 $\text{g m}^{-2} \text{d}^{-1}$, respectively. The average concentrations obtained were 32.6, 29.7, 26.1 and 26.4 mg L^{-1} for the influent and 9.6, 10.2, 9.7 and 15.4 mg L^{-1} for the effluent in the MBBR/SAF system. The average inlet and outlet concentrations resulted, and the respectively removal efficiency are shown in Table 4.12.

Table 4.12- Ammonia inlet and outlet average concentrations and respectively removal efficiency, at OLRs applied.

| OLR (g m ⁻² d ⁻¹) | N-NH ₄ ⁺ mg L ⁻¹ | | Removal |
|---|---|-------------|-----------|
| | In | Out | |
| 6 | 32.6 ± 6.37 | 9.6 ± 9.47 | 73 ± 24 % |
| 8 | 29.7 ± 6.03 | 10.2 ± 4.90 | 65 ± 16 % |
| 12 | 26.1 ± 5.44 | 9.7 ± 8.26 | 65 ± 22 % |
| 16 | 26.4 ± 4.64 | 15.4 ± 5.48 | 42 ± 25 % |

Fig. 4.5 shows the variation of inlet and outlet for ammonia concentration for four stages applied. The highest removal efficiency was obtained at stage 3, however when increased the organic load to 16 g m⁻² d⁻¹, a significant decrease of nitrification rate was observed.

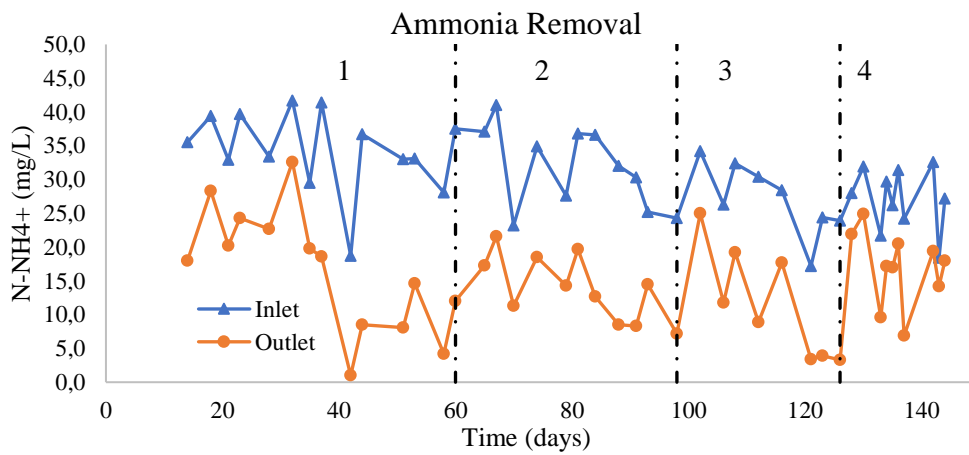


Figure 4.5- Inlet and Outlet of ammonium concentrations at different OLRs. Stage 1 – day0 to 60, stage 2 – day 61 to 98, stage 3- day 98 to 126 and stage 4- day 127 to 144

It was obtained surface organic loads of 0.69, 0.86, 1.10 and 1.46 g N-NH₄⁺ m⁻² d⁻¹ for ammonia at 6, 8, 12 and 16 g m⁻² d⁻¹ organic loads. (Table 4.13)

Table 4.13- N-NH₄⁺ surface loading rate (g N-NH₄⁺ m⁻² d⁻¹) at different OLRs.

| OLR (g m ⁻² d ⁻¹) | Ammonia loadings g N-NH ₄ ⁺ m ⁻² d ⁻¹ |
|---|--|
| 6 | 0.69 ± 0.13 |
| 8 | 0.86 ± 0.16 |
| 10 | 1.10 ± 0.22 |
| 13 | 1.46 ± 0.25 |

The nitrification removal rates obtained for the organic loads applied were, 0.33 ± 0.14 , 0.48 ± 0.12 , 0.63 ± 0.19 and 0.55 ± 0.21 g N-NH₄⁺ m⁻² d⁻¹ at stage 1, 2, 3 and 4.

Fig 4.6 shows the superficial load applied and removed for different organic loads applied, where the bisector line means 100% removal efficiency. The results showed that the removal rate decreases as ammonia loading was increased. Thus nitrification, in the present conditions, higher removal rates were achieved for loading rates up to 1.10 g N-NH₄⁺ m⁻² d⁻¹.

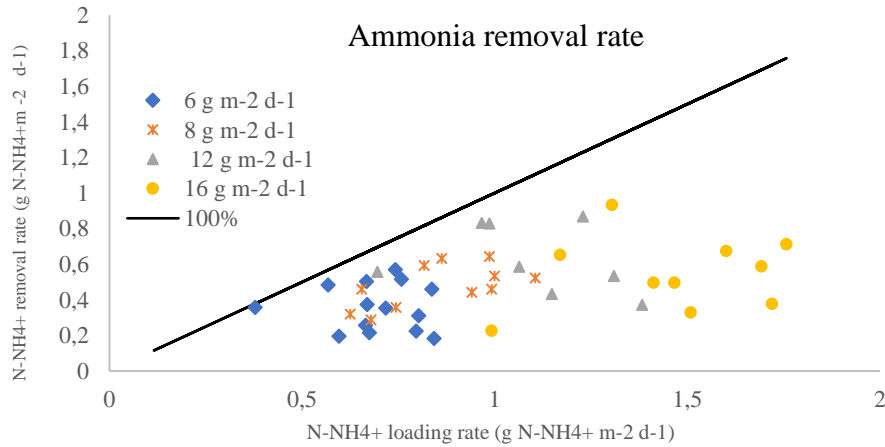


Figure 4.6- Amonia removal rate as function of amonia loads. For different OLRs applied.

Comparing biomass density with nitrification process, it was noticed that the reduced ammonia oxidation yield occurred despite the biomass growth detected in response to the increased loading. However, many studies had demonstrated that ammonia removal rates can be achieved at higher biomass concentrations. This finding suggests that, for high loading conditions, the diffusive substrate transport through the biofilm and other factors (temperature, O₂ concentration, etc.) are limiting the ammonia removal [27].

High removal efficiencies were achieved for ammonia removal, ranging from 73% to 42%, when surface organic loads for total COD were 5.2 to 2.17 gCOD m⁻² d⁻¹. Many studies had demonstrated that ammonia removal rates can be achieved at higher biomass concentrations. According to Andreottola, et al. 1998,[30] at total COD loads ranging from 100 to 500 g tCOD m⁻² d⁻¹ ammonia removal rates from 80% to 90% were achieved.

As already mentioned, the reactor used in this work, was designed for a $6 \text{ g COD m}^{-2} \text{ d}^{-1}$ loading rate capacity and to have three compartments, where the organic removal was supposed to occur in the first and second one and the nitrification in the third.

Higher organic loads had a detrimental effect on nitrification because the organic matter concentration that reached the cell 3 of the reactor was high. To enhance the performance of ammonia removal, larger volume of reactor would be required.

4.1.5 EPS quantification

The performance study of MBBR/SAF reactor was also evaluated as function of total EPS quantification. Fig. 4.7 and 4.8 shows the variation of concentration of proteins and carbohydrates in function of time, respectively. It was observed that EPS concentration decrease when flow rate was increased.

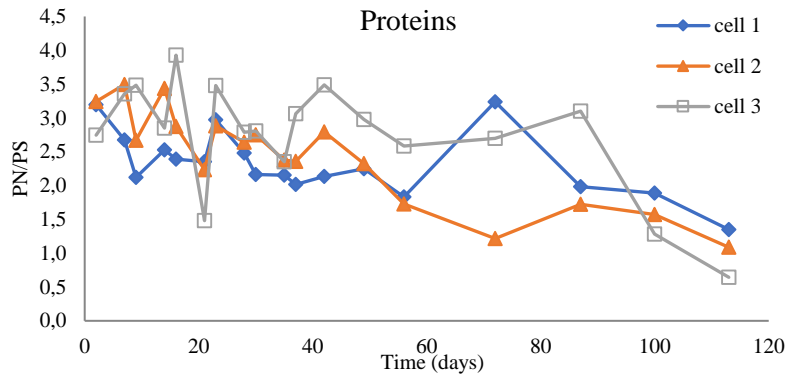


Figure 4.7- Proteins quantification evaluated as function of time, expressed at the specific weight, mgPN/gMLVSS

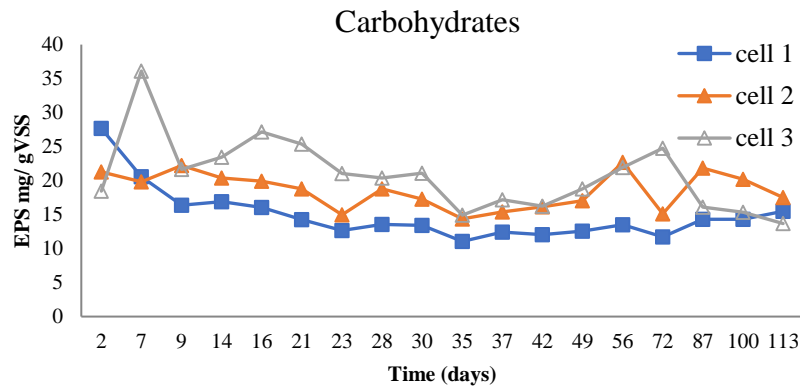


Figure 4.8- Carbohydrates quantification evaluates as function of time, at the specific weight mgPS/gMLVSS

An increase biomass density as organic load was increasing was observed, meaning that the attached biofilm was still consuming pollutants from the water and increasing the thickness of the biofilm. When dense thicknesses of biofilm were achieved, consumption rate and substrate transport were limited because of diffusion limitations in the deepest regions of the biofilm. This limitation can be one of the reasons for EPS decreasing.

4.2 External Mass Transfer coefficient determination

Batch tests were performed in order to evaluate the external mass transfer coefficient at different mixing intensities, for Media 1, Media 2 and Media 3. The DO concentration was fixed ranging from 2.5-3.5 mg L⁻¹ and mixing intensity controlled by balance air and nitrogen flow. The sCOD consumption by the biofilm at each mixing condition as function of time are illustrated in Appendix IV. For each media, the experimental removal rates (r_{exp}) were obtained from the slope of the linear regression when values of substrate concentrations as function of time were plotted. (Fig.4.9)

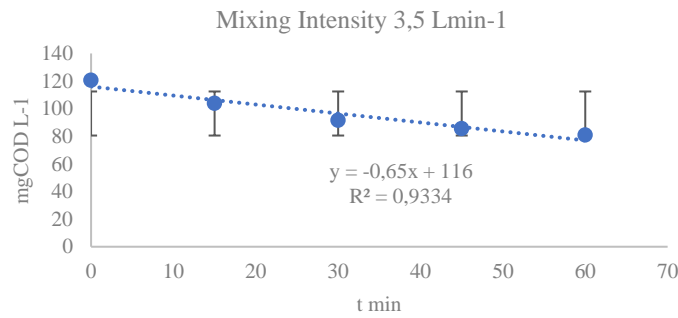


Fig. 4.9-a

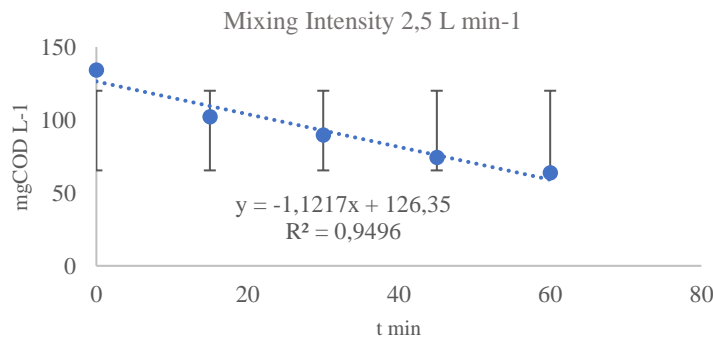


Fig. 4.9- b

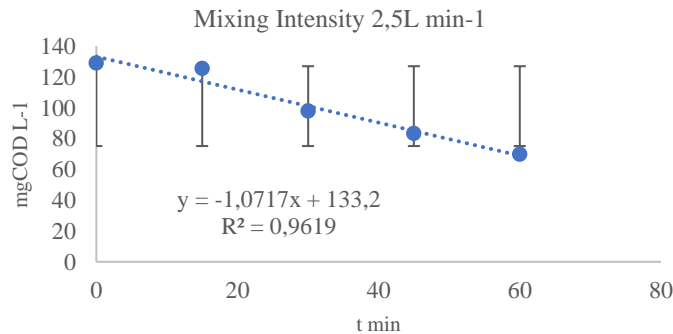


Fig. 4.9-c

Figure 4.9- Difference of sCOD concentration obtained as function of time, for Media 1(4.9- a), Media2 (4.9-b) and Media 3 (4.9-c) for the lowest mixing intensity.

The sCOD concentration obtained from Media 1, 2 and 3 at different mixing intensities are illustrated in Table 4.14. For Media 1, the mixing intensity applied were 3.5, 5, 7.5, 10, 20 and 30 $\text{L L}^{-1} \text{min}^{-1}$, for Media 2 were 2.5, 3.5, 5, 7.5, 10, 20 and 30 $\text{L L}^{-1} \text{min}^{-1}$ and, for Media 3 were 2.5, 3.5, 5, 10, 20 and 30 $\text{L L}^{-1} \text{min}^{-1}$. At the lowest mixing intensity, the r_{exp} obtained for Media 1, Media 2 and Media 3 were 39, 67.3 and 64.3 $\text{mg L L}^{-1} \text{min}^{-1}$, respectively and at the higher mixing intensity were 95.8, 111.20 and 99.8 $\text{mg L L}^{-1} \text{min}^{-1}$.

Comparing removal efficiencies of the different trials, within the range studied in these experiments, the difference between the minimum and the maximum removal rate achieved were about 29%, 35% and 15% for Media 1, Media 2 and Media 3, respectively.

Table 4.14- Removal rates obtained at different mixing intensities for Media 1, 2 and 3.

| Gas Flow Rate L min^{-1} | Mixing Intensity $\text{L L}^{-1} \text{min}^{-1}$ | $r_{\text{exp}} (\text{mg L}^{-1} \text{h}^{-1})$ | | |
|--------------------------------------|---|---|---------|---------|
| | | Media 1 | Media 2 | Media 3 |
| 2.5 | 0.07 | - | 67.30 | 64.30 |
| 3.5 | 0.10 | 39.00 | 73.70 | 72 |
| 5 | 0.14 | 55.20 | 103.40 | - |
| 7.5 | 0.21 | 60.80 | 117.90 | 84.6 |
| 10 | 0.28 | 55.00 | 112.80 | 84.2 |
| 15 | 0.42 | 83.20 | - | 92 |
| 20 | 0.56 | - | 105 | 87.4 |
| 25 | 0.69 | 95.80 | - | - |
| 30 | 0.83 | - | 111.32 | 99.8 |

From the results obtained on the different mixing intensities, was possible to verify that sCOD removal increase with the increasing mixing intensities until a maximum value, where sCOD conversion was no longer affected by mixing intensity.

The methodology applied for determination of mass transfer coefficient (K_{O_2}), required the calculation of the removal rate without external mass transfer resistance ($\text{L L}^{-1} \text{min}^{-1}$).

The removal rate with external mass transfer resistance (R) obtained from Media 1, Media 2 and Media 3 were 60,80, 103.4 and 84.6 $\text{mg L}^{-1} \text{h}^{-1}$, respectively at mixing intensities of 0.21, 0.14 and 0.21 $\text{L L}^{-1} \text{h}^{-1}$, respectively. (Fig. 4.10)

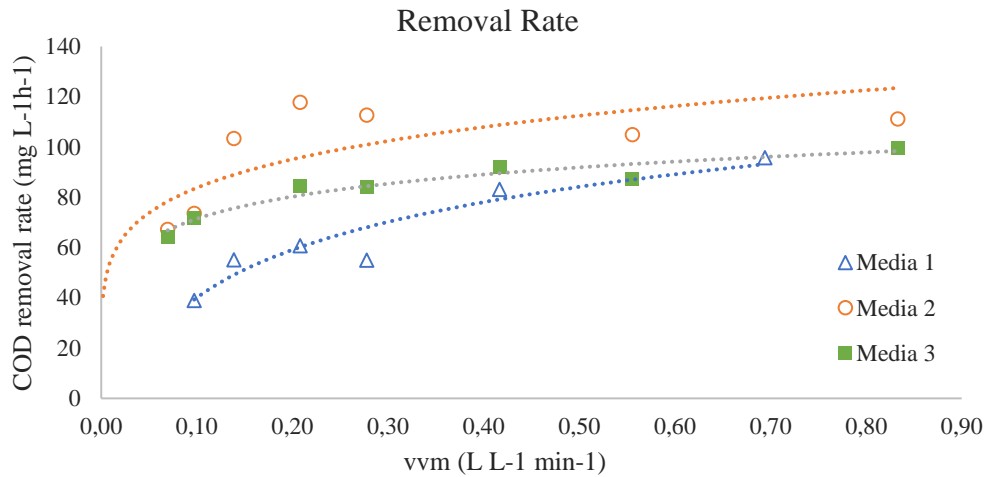


Figure 4.10 – COD Removal rates obtained as function of vvm for Media 1, Media 2 and Media 3 .

The boundary layer thickness and external mass transfer coefficient were evaluated by the method described in Appendix I. The influence of the mixing intensity on the estimated boundary layer thickness is illustrated in Fig. 4.11.

The mixing intensities, where effect of external mass transfer was observed, were ranging from 0.07- 0.21 L L⁻¹ min⁻¹. A linear correlation between the mixing intensity on the estimated boundary layer thickness was found.

The boundary layer obtained from Media 1 at 0.21 L L⁻¹ min⁻¹ was 35.5 μ m, from Media 2 at 0.14 L L⁻¹ min⁻¹ was 11.14 μ m and for Media 3 at 0.21 L L⁻¹ min⁻¹ was 10.94 μ m. It was revealed that the boundary layer thickness decreased as the mixing intensity was increased.

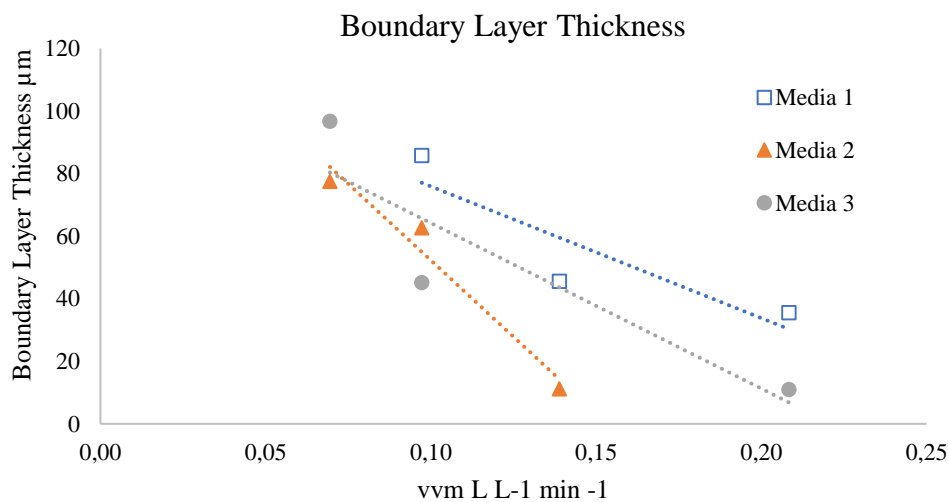


Figure 4.11- Boundary layer thickness obtained from Media 1,2 and at different mixing intensities, when sCOD conversion is no longer affected by mixing intensity.

During the experimental, the biofilm thickness was determined with the OCT microscope. The average biofilm thickness obtained from Media 1, Media 2 and Media 3 was 350.0, 155.83 and 187.23 μm . Figure 4.12 illustrate a scan image obtained from OCT microscope, from Media 2. In Appendix V, is shown images of medias analysed in this experimental work.

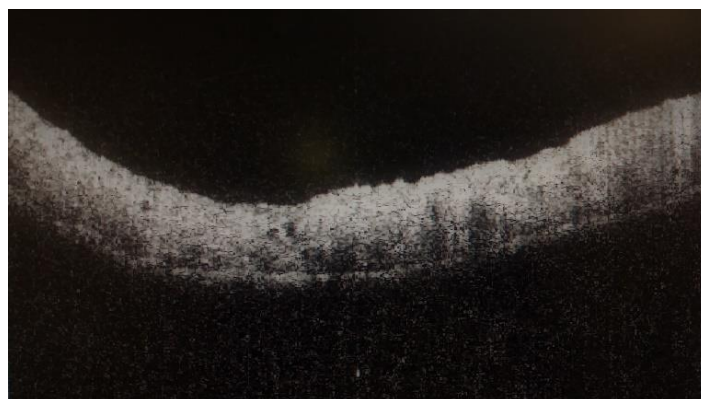


Figure 4.12- Scan imagine obtained from OCT microspipe for measumene of biofilm tkiness.

Fig. 4.13 represents the external mas transfer coefficient evaluated in function of mixing intensity for Media 1, Media 2 and Media 3, ranging from 0.07 to 0.21, where mass transfer is influenced by mixing intensity. The mass transfer results obtained from Media 1 at mixing intensities of 0.10, 0.14, and 0.21 $\text{L}^{-1}\text{min}^{-1}$ were 2.02, 3.82, and 4.89 m d^{-1} , from Media 2 at mixing intensities of 0.07, 0.10 and 0.14 $\text{L}^{-1}\text{min}^{-1}$ were 2.24, 2.77 and 15 m d^{-1} and, from Media 3 at mixing of 0.07, 0.10 and 0.21 $\text{L}^{-1}\text{min}^{-1}$ were 1.80, 3.84 and 15.90 m d^{-1} .

It was showed that the external mass transfer coefficient was increasing with mixing. From the experimental data presented, Media 2 showed that external mass transfer was lower, following by Media 1 and Media 3. The higher the external mass transfer coefficient lower the boundary layer, i.e. the higher the removal efficiency.

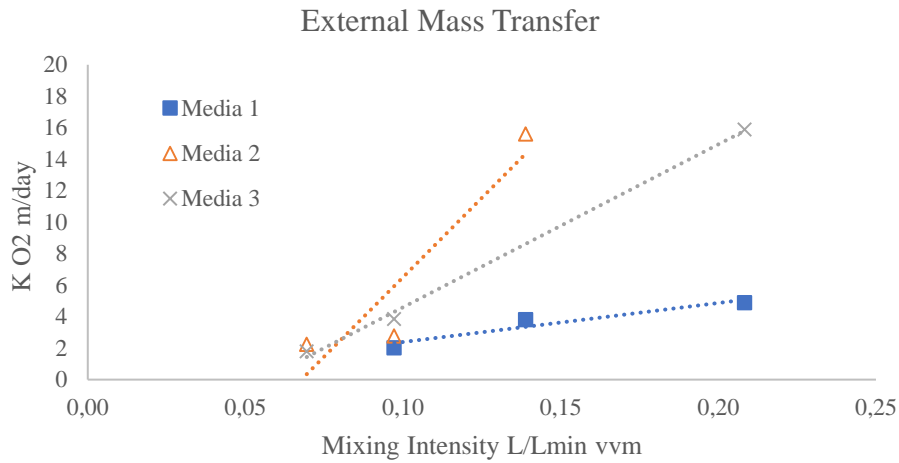


Figure 4.13- External Mass Transfer obtained from Media 1, Media 2 and Media 3.

Table 4.15 shows the obtained ranges of the factors mentioned, when the external mass transfer is influenced by mixing intensity.

For Media 1, r_{exp} within the range of 39.0- 60.80 mg L⁻¹ h⁻¹, a transfer coefficient range within the range of 2.77- 4.89 m d⁻¹ and a boundary layer within the range of 35.53 - 85.81 μm was achieved.

For Media 2 and Media 3 the r_{exp} obtained was ranging between 67.3- 103.4 mg L⁻¹ and 64.3- 84.6 mg L⁻¹ h⁻¹, respectively, the boundary layer was ranging between 11.14 – 77.50 μm and 10.95 – 96.73 μm , respectively, and the external mass transfer coefficient was ranging between 2.24 – 15.61 m d⁻¹ and 1.80 – 15.90 m d⁻¹, respectively.

The removal rates represented, as already mentioned, were gathered from the difference between the minimum and the maximum removal rate at the same conditions, which represents the influence of external mass transfer in substract consumption processes.

Table 4.15- Summary of the results obtained from three different medias, for sCOD removal, Mass transfer, Boundary layer and removal efficiency.

| Range | Media 1 | Media 2 | Media 3 |
|---|--------------|--------------|-------------|
| r rexp (mg L⁻¹ h⁻¹) | 39.0 – 60.80 | 67.3 – 103.4 | 64.3 – 84.6 |
| Mass transfer coefficient m d⁻¹ | 2.8 – 4.9 | 2.24 -15.6 | 1.8 – 15.9 |
| Boundary Layer μm | 35.53 – 85.8 | 11.14 -77.5 | 11.0 – 96.7 |
| Removal % | 29% | 35% | 15% |

For an average mixing ranging from 0.07 to 0.21 L⁻¹min⁻¹ (i.e. where mass transfer is strongly influenced by mixing intensity), the average boundary layer thickness obtained ranging from 35.53 to 85.8 μm, 11.14 to 77.5 μm and 11.0 to 96.7 μm, for Media 1, Media 2 and Media 3, respectively.

The average thickness of the biofilm attached from Media 1 obtained through scan images showed that this media presented higher thickness regarding Media 2 and Media 3. Higher thickness can lead limitations substrate rate consumptions, hence higher boundary layer.

Comparing Media 2 with Media 3, the biomass density obtained was 155.83 μm and 187.23 μm, respectively. As the biofilm density was in the same range for both, the parameter that could be affected the removal efficiency can be related with shape and size of the media.

It was also evaluated the diffusion oxygen coefficient for each media. The oxygen mass diffusivity coefficient is a proportionality constant between the molar flux due to molecular diffusion and the gradient in the concentration of the species. The higher the diffusivity, the faster the diffusion between the species, into each other. The obtained results were 0.78, 2.40 and 0.28 m² d⁻¹. Media 2 showed the highest diffusivity, compared with Media 1 and 2, as expected.

This page was intentionally left blank

5. Conclusion

The research study evaluated the performance of pilot-scale MBBR/SAF reactors at relatively high organic loading rates. Thus, the efficiency of organic matter and ammonia removal was investigated to understand what the maximum loading rate that could be applied was. In parallel, other parameters such as solids removal, biomass density growth and EPS were evaluated.

It was clearly shown that the MBBR/SAF in the present conditions, the organic load where high efficiencies were obtained, i.e. at organic load of $12 \text{ g m}^{-2} \text{ d}^{-1}$ the obtained results were for soluble BOD, removal efficiency ranging from $92 \pm 4\%$, corresponding to surface loading rate of $2.35 \pm 0.8 \text{ g BOD m}^{-2} \text{ d}^{-1}$, and removal rate of $0.57 \pm 0.21 \text{ g BOD m}^{-2} \text{ d}^{-1}$.

For ammonia removal above of $0.69 \text{ g N NHH}_4^+ \text{ m}^{-2} \text{ d}^{-1}$ an average removal efficiency of $42\% \pm 25$ was achieved, while for $8 \text{ g m}^{-2} \text{ d}^{-1}$ an average removal efficiency of $65\% \pm 22$ was achieved.

The decrease of the removal rate efficiency can be related to the diffuse substrate transport processes, since the biomass density grew as OLR was increased. The solids removal for a MBBR/SAF reactor low removal efficiency because the reactor worked without recirculation of sludge and with a low HRT. It was observed that the biofilm surface density evaluation over time was related with organic loads applied.

For the aeration intensities used, the external mass transfer coefficient and boundary layer thickness and obtained ranged from $2.77 - 4.90 \text{ m d}^{-1}$ and $35.53 - 85.81 \text{ }\mu\text{m}$ for Media 1, from $2.24 - 15.61 \text{ m d}^{-1}$ and $11.14 - 77.5 \text{ }\mu\text{m}$ for Media 2 and, from $1.80 - 15.90 \text{ m d}^{-1}$ and $11.0 - 96.73 \text{ }\mu\text{m}$ for Media 3, respectively.

The obtained results showed higher mass transfer coefficient and smaller boundary layer for Media 2, suggesting that at surface area of the mentioned media, $220 \text{ m}^2 \text{ m}^{-3}$ the mechanism of diffusion in mass transfer processes were more suitable than Media 1 and Media 3.

This page was intentionally left blank

6. References

- [1] S. Sehar and I. Naz, "Role of the Biofilms in Wastewater Treatment," *INTECH*, vol. Chapter 7, no. [Consult. 19 Settembre 2017], pp. 122–139, 2016.
- [2] Department of economic and social Affairs, "World Water Day," *United Nations*, 2017. [Online]. Available: <https://www.un.org/development/desa/en/news/sustainable/world-water-day-2017-why-waste-water.html>. [Accessed: 10-Sep-2017].
- [3] M. Samer, "Biological and Chemical Wastewater Treatment Processes," vol. 1, no. [Consult. 10 Settembre 2017]), pp. 1–50, 2015.
- [4] A. Barwal and R. Chaudhary, "To study the performance of biocarriers in moving bed biofilm reactor (MBBR) technology and kinetics of biofilm for retrofitting the existing aerobic treatment systems : a review," *Env. Sci Biotechnol*, vol. 13, no. [Consult. 19 Settembre 2017], pp. 285–299, 2014.
- [5] R. P. Borkar, M. L. Gulhane, and A. J. Kotangale, "Moving Bed Biofilm Reactor – A New Perspective in Wastewater Treatment," *IOSR J. Environ. Sci.*, vol. 6, no. [Consult. 2 Settembre 2017], pp. 15–21, 2013.
- [6] Metcalf & Eddy, *Wastewater Engineering: Treatment and Reuse*, 4th ed. McGraw-Hill, 2003.
- [7] M. B. Pescod, "Wastewater treatment," *FAO corporate document repository*. [Online]. Available: <http://www.fao.org/docrep/t0551e/t0551e05.htm>. [Accessed: 19-Sep-2017].
- [8] WPL- Environmental Wastewater Problems solutionns, "Primary treatment options," 2017. [Online]. Available: <https://www.wplinternational.com/solution-types/municipal-wastewater-treatment/primary-treatment-options-municipal-wastewater-treatment/>. [Accessed: 30-Aug-18].
- [9] "Primary Wastewater Treatment- City of Guelph," *City Guelph*, no. Accessed September 19, 2017, pp. 1–17.
- [10] US Environmental Protection Agency, "Wastewater Treatment Works... The Basics," *United States Environ. Prot.*, no. Accessed September 19, 2017, 1998.
- [11] J. M. S. Dias, "A state-of-the-art review and market prospect of MBBR and SAF technologies using buoyant plastic media," Cranfield University, 2014.
- [12] WaterWorld, "Wastewater," *PennWell Corporation*, 2017.
- [13] J. P. McQuarrie and J. P. Boltz, "Moving Bed Biofilm Reactor Technology: Process

- Applications, Design, and Performance,” *Water Environ. Res.*, vol. 83, no. 6, pp. 560–575, Jun. 2011.
- [14] E. Loupasaki and E. Diamadopoulos, “Attached growth systems for wastewater treatment in small and rural communities: a review,” *J. Chem. Technol. Biotechnol.*, vol. 88, no. 2, pp. 190–204, Feb. 2013.
- [15] A. Jácome, J. Molina, R. Novoa, J. Suárez, and S. Ferreiro, “Simultaneous carbon and nitrogen removal from municipal wastewater in full-scale unaerated/aerated submerged filters,” *Water Sci. Technol.*, vol. 69, no. 1, p. 217, Jan. 2014.
- [16] B. L. Nogueira, P. Julio, and A. R. Secchi, “Determination of the external mass transfer coefficient and influence of mixing intensity in moving bed biofilm reactors for wastewater treatment,” *elsevier*, no. September 19, 2017, p. 9, 2015.
- [17] J. Maria and F. Ramos, “Determinação de Parâmetros Cinéticos de Biofilmes formados por *Pseudomonas fluorescens*,” Universidade do Porto, 2008.
- [18] J. Kloc, T. Camesano, R. Thompson, and O. Sponsor, “The Study of Biological Wastewater Treatment through Biofilm Development on Synthetic Material vs . Membranes,” Worcester Polytechnic Institute, 2012.
- [19] K. Sauer, “The genomics and proteomics of biofilm formation,” *Genome Biol.*, vol. 4, no. 6, p. 219, 2003.
- [20] iGEM, “Modeling - Simulating biofilm formation and the stratification of concentration of oxygen.” [Online]. Available: <http://2011.igem.org/Team:ZJU-China/bio-modeling.html>. [Accessed: 20-Sep-2017].
- [21] B. L. Nogueira, “REATORES DE LEITO MÓVEL COM BIOFILME - MODELAGEM MATEMÁTICA E ESTUDOS DE TRANSFERÊNCIA DE MASSA EM SISTEMAS COM CULTURAS MISTAS,” Instituto Alberto Luiz Coimbra de Pós-Graduação e Pesquisa de Engenharia, 2016.
- [22] A. Mašić, J. Bengtsson, and M. Christensson, “Measuring and modeling the oxygen profile in a nitrifying Moving Bed Biofilm Reactor,” *Math. Biosci.*, vol. 227, no. 1, pp. 1–11, Sep. 2010.
- [23] H. Odegaard, B. Rusten, and T. Westrum, “A new moving bed biofilm reactor - applications and results,” *Water Sci. Technol.*, vol. 29, no. 10–11, 1994.
- [24] H. Odegaard, “The influence of carrier size and shape in the moving bed biofilm process,” *Water Sci. Technol.*, vol. 41, no. 4–5, 1998.

- [25] “Determination of Total Suspended Solids (TSS) and Total Volatile Solids (TVS) in Waters of Fresh/Estuarine/Coastal Waters.”
- [26] The Laboratory People, “COD or Chemical Oxygen Demand definition,” *THE LABORATORY PEOPLE*, 2017. [Online]. Available: <http://camblab.info/wp/index.php/272/>. [Accessed: 16-Sep-2017].
- [27] A. Siciliano and S. De Rosa, “An experimental model of COD abatement in MBBR based on biofilm growth dynamic and on substrates’ removal kinetics,” *Environ. Technol.*, vol. 37, no. 16, pp. 2058–2071, Aug. 2016.
- [28] A. Siciliano and S. De Rosa, “Experimental formulation of a kinetic model describing the nitrification process in biological aerated filters filled with plastic elements,” *Environ. Technol. (United Kingdom)*, vol. 36, no. 3, pp. 293–301, 2015.
- [29] A. Aygun, B. Nas, and A. Berkay, “Influence of High Organic Loading Rates on COD Removal and Sludge Production in Moving Bed Biofilm Reactor,” vol. 25, no. 9, 2008.
- [30] G. Andreottola, P. Foladori, M. Ragazzi, and F. Tatàno, “Experimental comparison between MBBR and activated sludge system for the treatment of municipal wastewater,” *IWA Publ. 2000*, pp. 375–382, 1998.

This page was intentionally left blank

7. Appendix

7.1 Appendix I

External Mass Transfer Calculation

All the calculations related with external mass transfer coefficient were estimated by following the article ““Determination of the external mass transfer coefficient and influence of mixing intensity in moving bed biofilm reactors for wastewater treatment” by B. Nageire. The important formulations used in this study, is briefly describe the following section.

The r^{exp} for each experimental was obtained through the slope of the linear decrease plotted from values of acetate concentration (mg/L) as function of time. The experimental flux of the oxygen of the biofilm can be calculated by:

$$J_{O_2}^{exp} = r^{exp} * \gamma_{\frac{O_2}{substrate}} * \frac{V_{bulk}}{A}$$

Where,

$J_{O_2}^{exp}$ is experimental flux of oxygen of the biofilm;

r^{exp} is the experimental removal rate;

$\gamma_{\frac{O_2}{substrate}}$ is he stoichiometric factor between the oxygen and subtract uptake;

V_{bulk} is the volume of liquid inside;

A is the total surface area carriers within the reactor.

The flux of oxygen over the boundary layer can be calculated as function of the concentration difference between the liquid phase and the surface of the biofilm, and the external mass transfer. This is given by the following equation.

$$J_{O_2}^{BL} = k_{O_2} * (S_{O_2}^{bulk} - S_{O_2}^{interf})$$

Where,

$J_{O_2}^{BL}$ is the flux of oxygen over the boundary layer;

k_{O_2} is the external mass transfer coefficient;

$S_{O_2}^{bulk}$ is the liquid phase concentration;

$S_{O_2}^{interf}$ is the surface of the biofilm concentration.

The flux of the substrate over the surface of the biofilm is estimated when a zero-order approach for conversion in the biofilm is used, which can be describe by the following equation:

$$J_{O_2}^{Biof} = D_{O_2}^{biof} \frac{dS_{O_2}^{bulk}}{dz} = \sqrt{2D_{O_2}^{biof} q_{O_2,max} * X} * \sqrt{S_{O_2}^{interf}}$$

Where,

$J_{O_2}^{Biof}$ is the flux of substrate over the surface of the biofilm;

$D_{O_2}^{biof}$ is the oxygen diffusivity in the biofilm;

$q_{O_2,max}$ is the maximum substrate specific conversion rate;

X is the biomass density.

The removal rate without influence of external mass transfer is given by the following equation:

$$R = \frac{\frac{\sum r_{exp}}{\sigma^2}}{\sum 1/\sigma^2}$$

Where,

R is the removal rate without influence of external mass transfer;

σ^2 is the experimental variance.

When the influence of external mass transfer is negligible the fluxes $J_{O_2}^{exp}$ and $J_{O_2}^{Biof}$ and the concentrations $S_{O_2}^{interf}$ and $S_{O_2}^{bulk}$ were assumed equal, leading to the next equation:

$$R \gamma_{\frac{O_2}{substrate}} \frac{V_{bulk}}{A} = \sqrt{2D_{O_2}^{biof} q_{O_2,max} * X} * \sqrt{S_{O_2}^{bulk}}$$

The following equation describes the external mass transfer coefficient for each experiment.

$$k_{O_2} = \frac{V_{bulk}}{A} * \frac{r^{exp} * R^2}{R^2 - r^{exp2}} * \frac{\gamma_{\frac{O_2}{substrate}}}{S_{O_2}^{bulk}}$$

The boundary layer thickness is given by:

$$\delta = \frac{D_{O_2}^{water}}{k_{O_2}}$$

Where,

δ is the boundary layer thickness;

$D_{O_2}^{water}$ is the oxygen diffusivity in water.

This page was intentionally left blank

7.2 Appendix II

DO concentration, temperature and pH variation of the MBBR/SAF reactor as function of time.

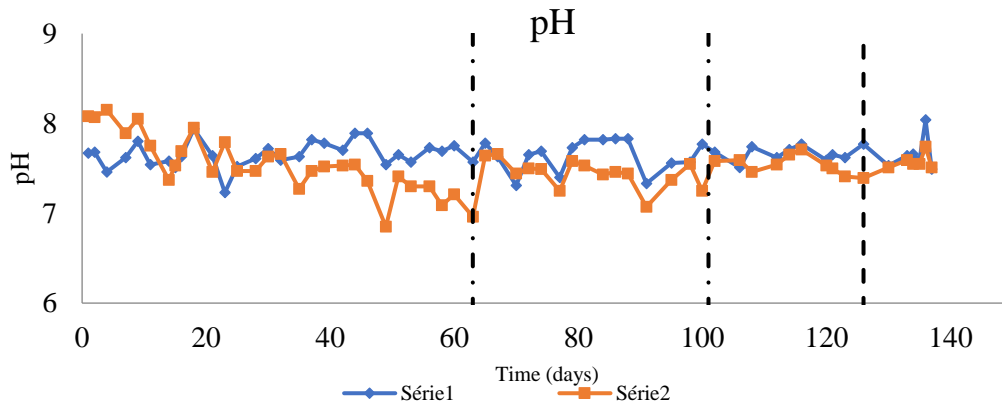


Figure 7.1- pH variation obtained for inlet and outlet at different OLRs.

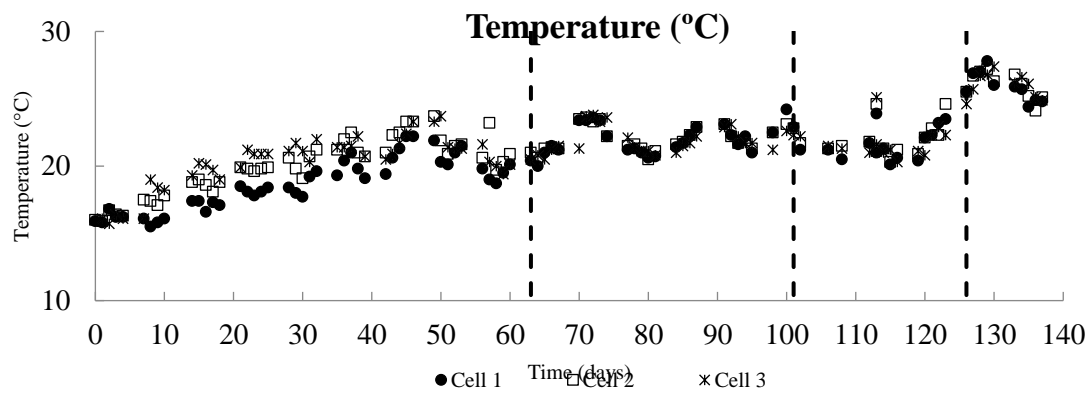


Figure 7.2- Evaluation of the temperature within the reactor for a frame time of six months, for cell 1, cell 2 and cell3.

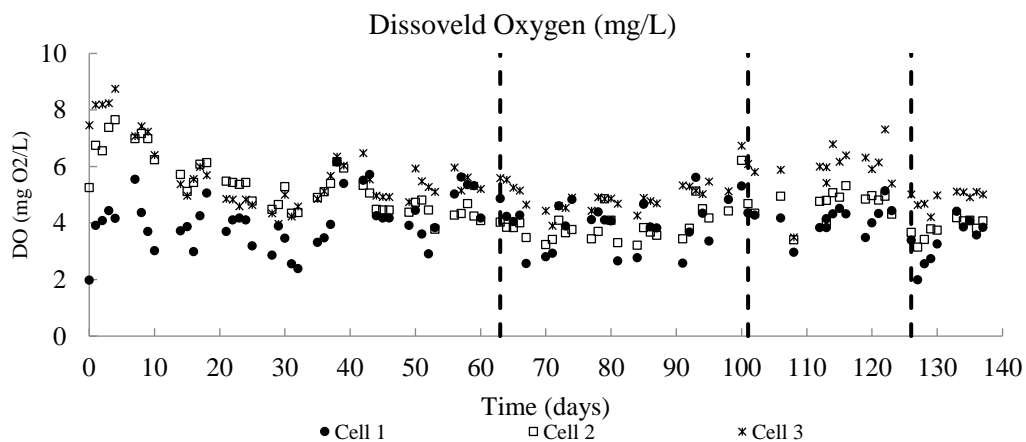


Figure 7.3- Dissoveltd Oxygen variation obtained for cell 1, cell 2 and cell 3, at different OLRs.

This page was intentionally left blank

7.3 Appendix III

Organic removal rate

- COD removal

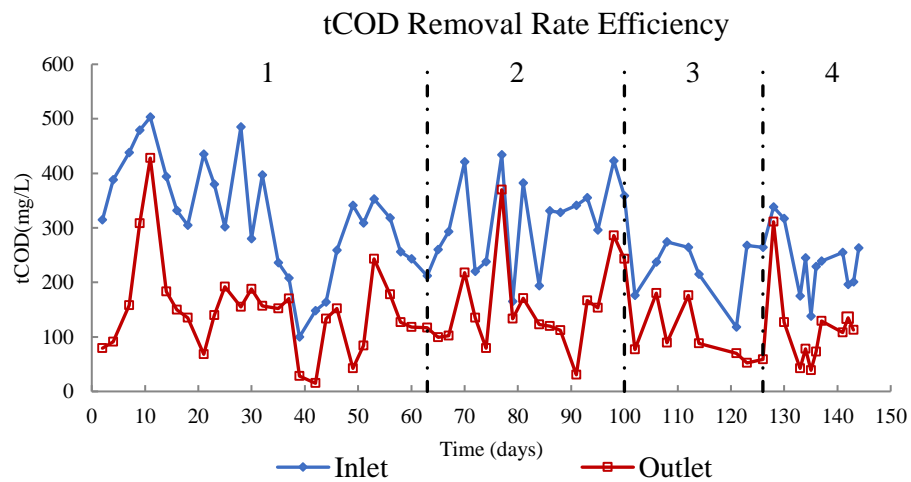


Figure 7.4- Total COD concentration removal efficiency (mgL^{-1}) versus time (days) for different OLRs. Stage 1 – day 0 to 63, stage 2 – day 64 to 100, stage 3- day 101 to 126 and stage 4- day 127 to 140.

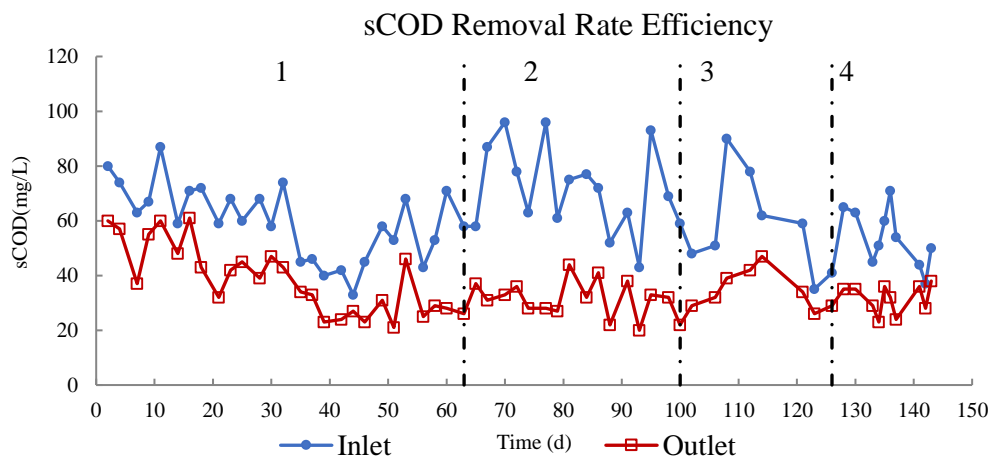


Figure 7.5- Soluble COD concentration removal efficiency (mgL^{-1}) versus time (days) for different OLRs. Stage 1 – day 0 to 63, stage 2 – day 64 to 100, stage 3- day 101 to 126 and stage 4- day 127 to 140.

- BOD

removal

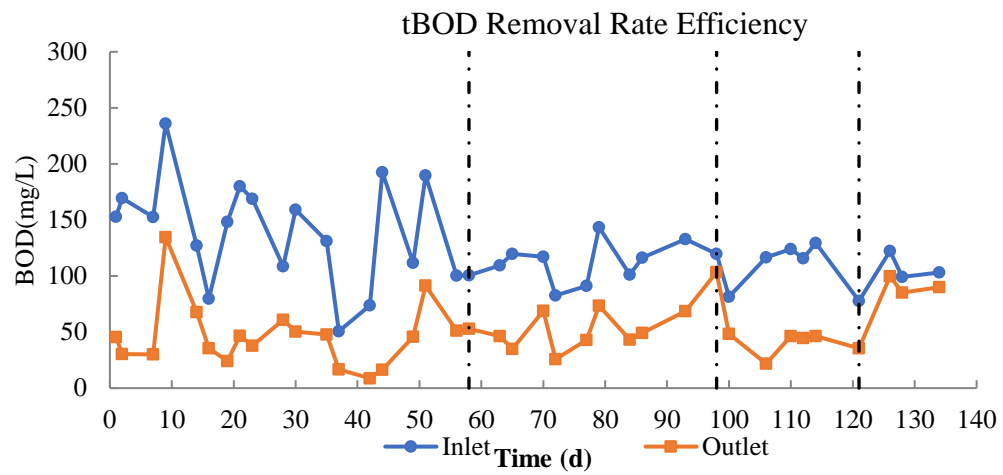


Figure 7.6 - Total BOD concentration removal efficiency (mgL^{-1}) versus time (days) at different OLRs. Stage 1 – day 0 to 58, stage 2 – day 59 to 98, stage 3- day 99 to 121 and stage 4- day 122 to 134.

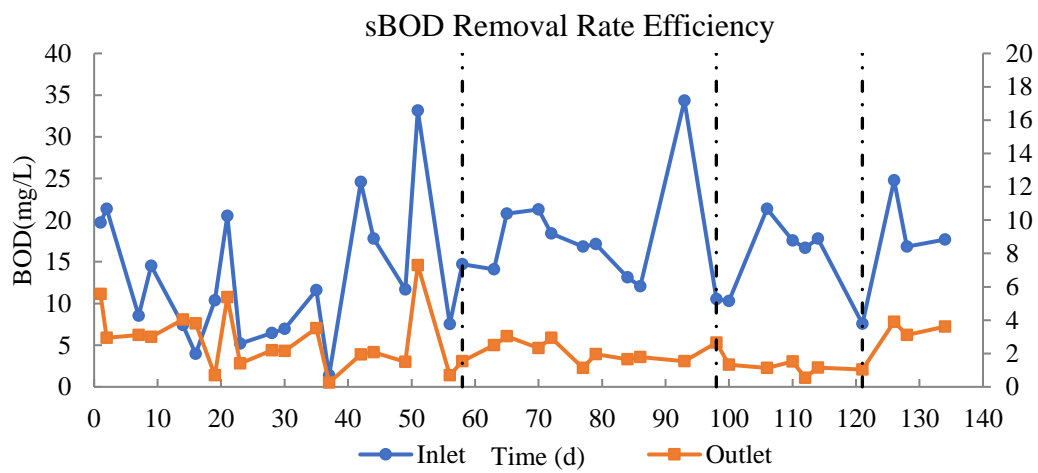


Figure 7.7- Total BOD concentration removal efficiency (mgL^{-1}) versus time (days) at different OLRs. Stage 1 – day 0 to 58, stage 2 – day 59 to 98, stage 3- day 99 to 121 and stage 4- day 122 to 134

7.4 Appendix IV

External Mass transfer results

Media 1 – COD removal rate in function of time for different mixing intensity applied.

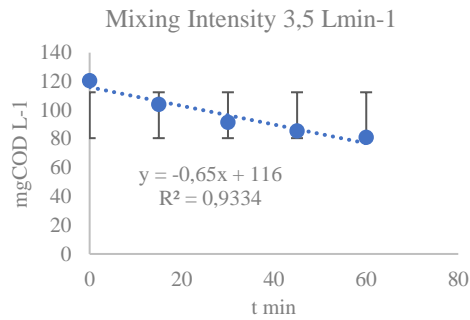


Fig.7.8-a

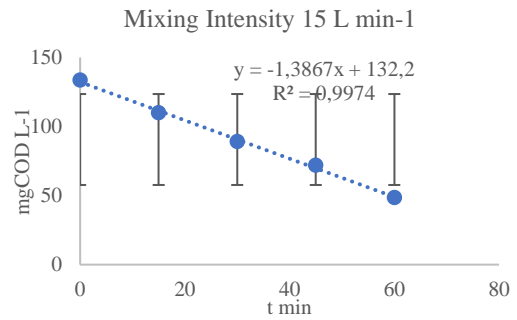


Fig. 7.8-e

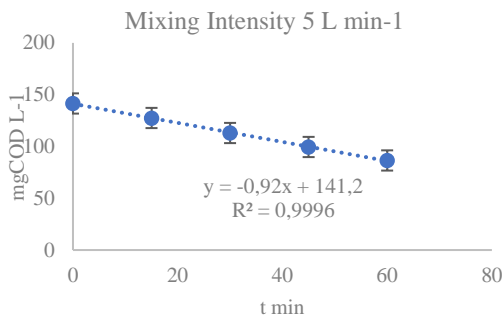


Fig. 7.8-b

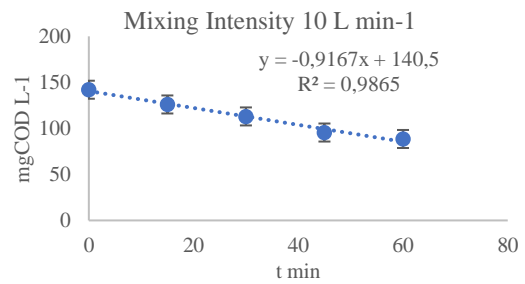


Fig. 7.8-d

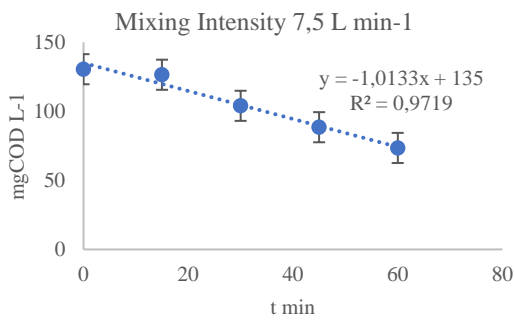


Fig. 7.8-c

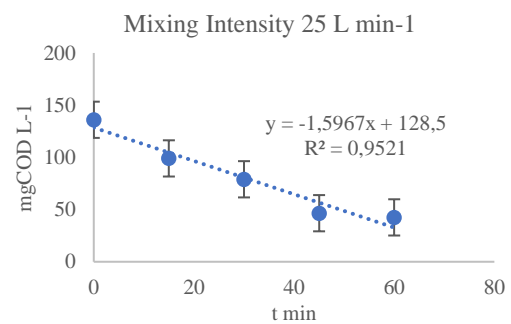


Fig. 7.8-f

Figure 7.8- Difference of sCOD concentration obtained as function of time, for Media 1 at different mixing intensities 3.5 vvm Fig.7.8- a, 5 Fig.7.8- b, 7.5 vvm Fig.7.8- c, 10 vvm Fig.7.8- d, 15 vvm Fig.7.8- e, 25vvm Fig.7.8- f.

Media 2 – COD removal rate in function of time for different mixing intensity applied.

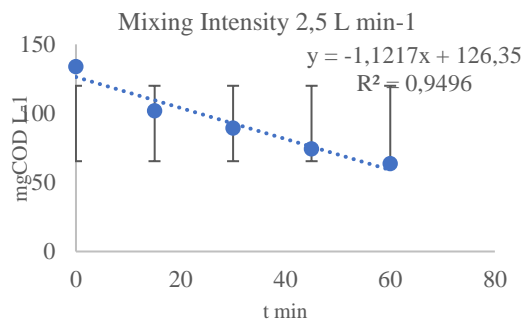


Fig. 7.9 – a

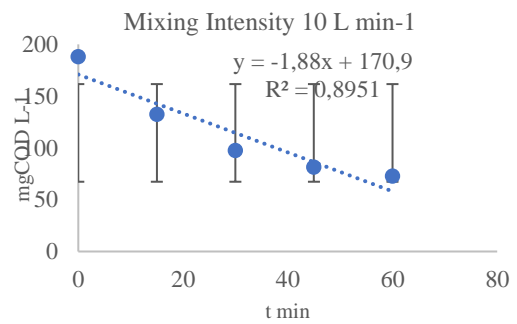


Fig. 7.9 – e

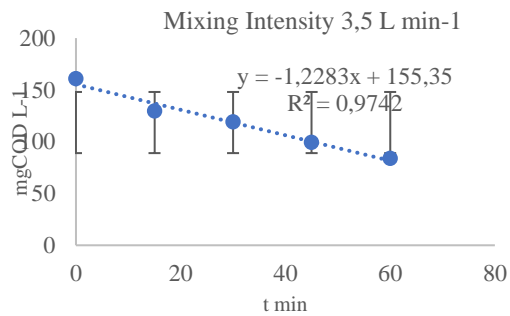


Fig. 7.9 – b

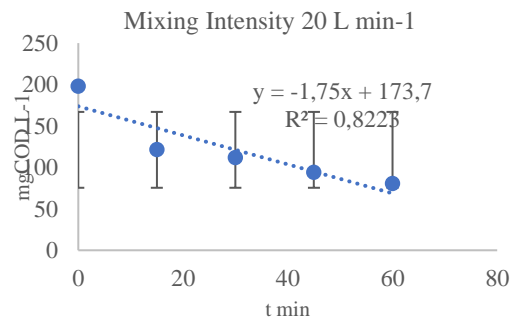


Fig. 7.9 – f

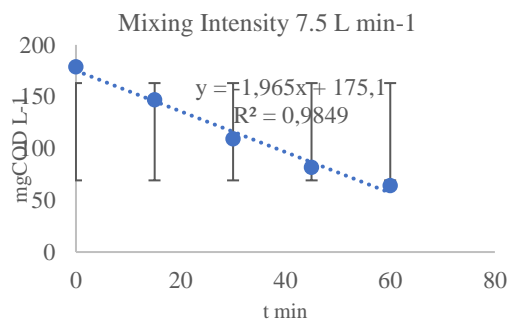


Fig. 7.9 – c

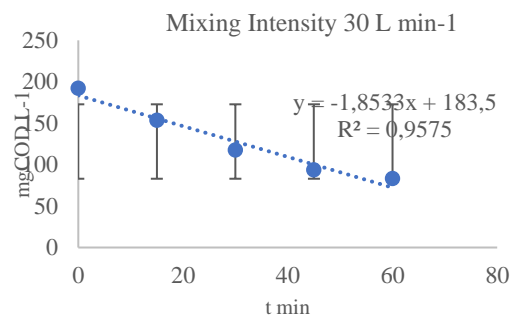


Fig. 7.9 – f

Figure- 7.9 Difference of sCOD concentration obtained as function of time, for Media 2 at different mixing intensities 2.5 vvm Fig.7.9 – a, 3.5 vvm Fig.7.9- b, 10 Fig.7.9- c, 15 vvm Fig.7.9- d, 20 vvm Fig.7.9- e, 30 vvm Fig.7.9-f.

Media 3 – COD removal rate in function of time for different mixing intensity applied.

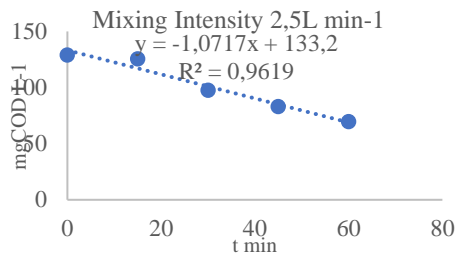


Fig. 31 - a

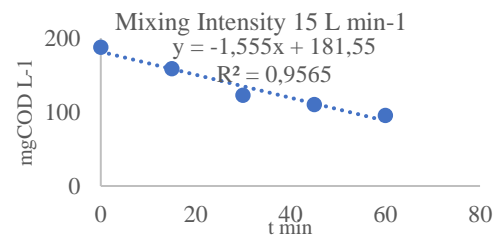


Fig. 31 - e

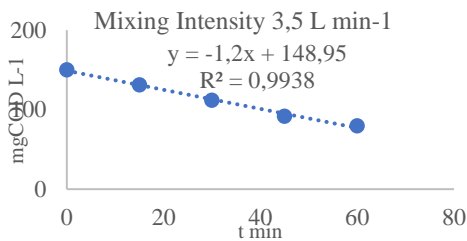


Fig. 31 - b

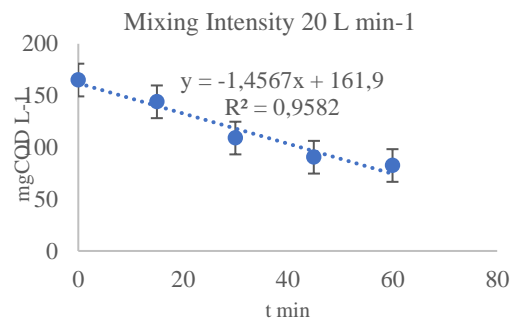


Fig. 31 - f

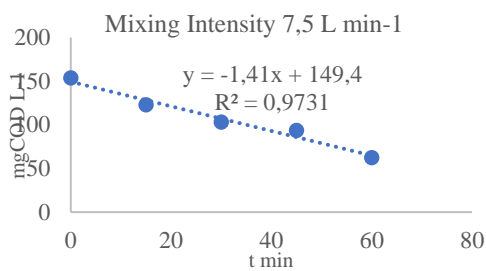


Fig. 31 - c

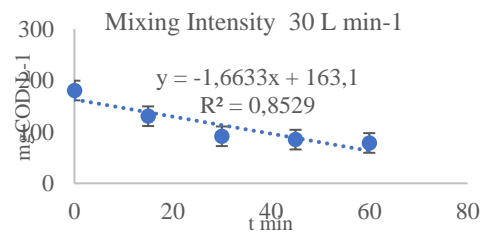


Fig.

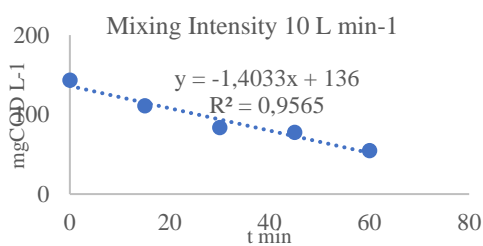


Fig. 31 - d

Figure 31- Difference of sCOD concentration obtained as function of time, for Media 1 at different mixing intensities 2.5 vvm Fig.31 - a, 3.5 vvm Fig.31- b, 7.5 vvm Fig.31- c, 10 vvm Fig.31- d, 15 vvm Fig.31- e, 20 vvm Fig.31-f and 30 vvm Fig.31-g.

This page was intentionally left blank

7.5 Appendix V

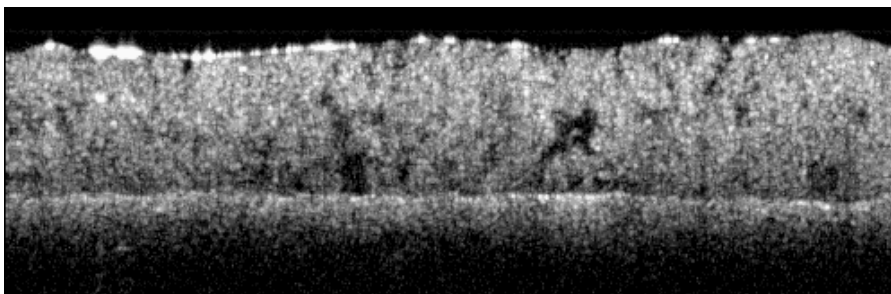


Fig. 7.10-a

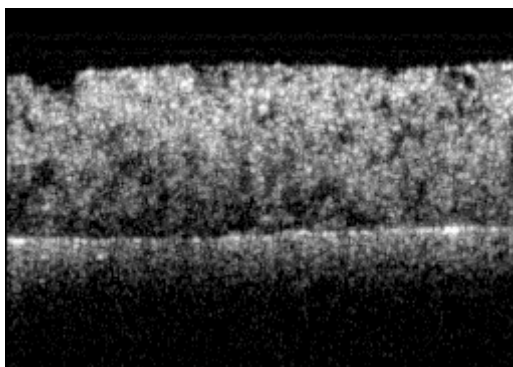


Fig. 7.10-b

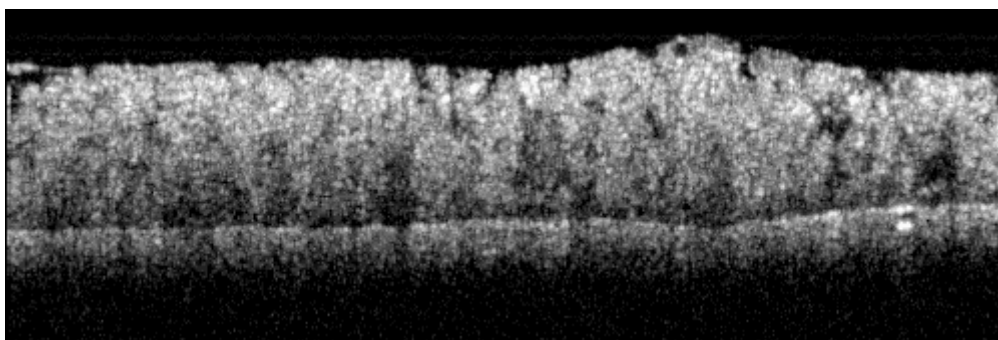


Fig. 7.10-c

Figure 7.10- Examples of scan images obtained for biofilm thickness measurements. Fig. 7.10-a, Fig. 7.10-b and Fig. 7.10-c



Figure 7.11- Attached biomass Media 1



Figure 7.12- Attached biomass Media 2.



Figure 7.13- Attached biomass Media 3.



Figure 7.14- Lab scale reactor with Media 3.